Coordination Chemistry Reviews 253 (2009) 2432–2449

Contents lists available at ScienceDirect

Coordination Chemistry Reviews

journal homepage: www.elsevier.com/locate/ccr

Review

Spin crossover complexes with N_4O_2 coordination sphere—The influence of covalent linkers on cooperative interactions

Birgit Weber*

Ludwig Maximilian University Munich, Department of Chemistry and Biochemistry, Butenandtstr. 5-13 (Haus F), D-81377 München, Germany

Contents

1. Introduction 2432
2. The ligand system 2433
3. The mononuclear building blocks 2434
   3.1. General trends 2434
   3.2. Influence of different molecules on the crystal packing 2436
   3.3. Understanding cooperative interactions 2437
   3.4. Photomagnetic properties 2438
4. From monomer to polymer systems 2438
   4.1. Increasing cooperative interactions 2438
   4.2. Effects of solvent molecules on the SCO behavior 2440
   4.3. Two-step versus single step spin transitions 2440
5. Dinuclear complexes 2442
6. Characterization in solution 2445
7. Conclusion and prospectives 2447
   Acknowledgements 2447
   References 2447

ARTICLE INFO

Article history:
Received 27 July 2008
Accepted 8 October 2008
Available online 14 October 2008

Keywords:
Iron
N, O ligands
Magnetic properties
Spin crossover

ABSTRACT

About 10 years ago Jäger and co-workers demonstrated the possibility of preparing an iron(II) spin crossover complex of a Schiff-base like N_2O_2 coordinating ligand in combination with imidazole or pyridine as axial ligands. Starting at this point, we have now prepared over 50 octahedral iron(II) complexes of this ligand type. Thirty of these new compounds are spin crossover complexes that can be subdivided into monomer (9), polymer (12) and dimer (9) systems. This review gives an overview of this complex class. Special consideration was given to the influence of covalent linkers on cooperative interactions during the spin transition, as the preparation of highly cooperative spin crossover complexes with wide thermal hysteresis loops around room temperature is still one of the major goals of a preparative chemist working in this area of research. In order to more closely evaluate the influence of the covalent linkers on the spin transition properties the complexes were not only investigated in the solid state but also in solution. For this purpose the proton NMR spectra of the complexes were analyzed in dependence on temperature and we will introduce the reader to the benefits of this method.

1. Introduction

Spin transition complexes (spin crossover, SCO) are an interesting class of compounds that can be switched between the paramagnetic high-spin (HS) and the diamagnetic low-spin (LS) state by external perturbations such as temperature, pressure or light [1]. Several applications in the field of information technology can be envisioned for this class of substance, especially for complexes that exhibit a wide hysteresis around room temperature (memory effect) [2]. Although spin crossover could be observed for any octahedral complex with d^n ($n = 4$–7) electron configuration, the spin transition in octahedral iron(II) complexes is by far the most thoroughly investigated with the diamagnetic low-spin state

* Tel.: +49 89218077772; fax: +49 89218077407.
E-mail address: bwmch@cup.uni-muenchen.de.

0010-8545/$ – see front matter © 2008 Elsevier B.V. All rights reserved.
doi:10.1016/j.ccr.2008.10.002

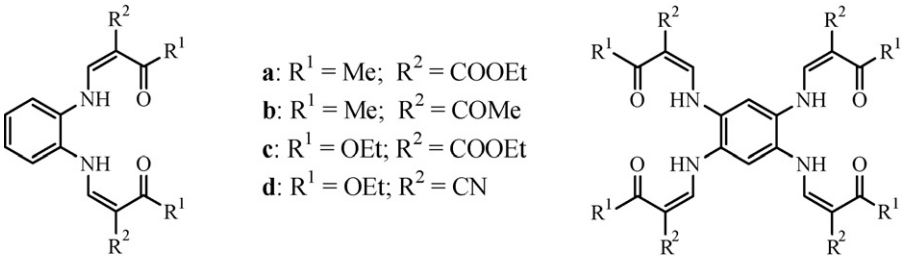

Scheme 1. Overview of the equatorial ligands, with their abbreviations, used in this work.

and the paramagnetic high-spin state. Of those complexes investigated, about 90% exhibit a N_6 coordination sphere [1], while other examples with a N_4O_2 [3], N_4S_2 [4], N_4C_2 [5] or $N_3C_2O_2$ [6] coordination sphere are rare. In contrast to this observation, there are several examples for iron(III) spin crossover complexes with N_4O_2 coordination sphere [1].

The influence of chemical parameters such as the ligand, counter-ions or solvent molecules on the spin transition, especially the transition temperature, $T_{1/2}$, is now well understood. This is not the case for cooperative effects between the molecules during the spin crossover phenomenon. The possibility to predict which effect is induced by a change of the ligand structure or other parameters is limited. The occurrence of hysteresis effects depends on the "communication" between the metal centers during the spin transition, the cooperative effects. Different intermolecular interactions such as π-stacking, hydrogen bonds or van der Waals interactions are suitable information transmitters. However, the application of covalent linkers as suggested by Kahn et al. [2a,7] did attract special attention over the last years as the spread of those interactions can be more easily controlled. This resulted in the synthesis and characterization of several iron(II) spin crossover coordination polymers [8] as well as dinuclear species [9]. The latter can be considered to be the simplest systems of spin-coupled polymers and the investigation of those systems provides fundamental information about intramolecular magnetic interactions and a possible synergy between those interactions and the SCO properties.

2. The ligand system

Over the last years in the Jäger research group, a ligand system was developed that can be subdivided into the three basic structures [10]. Type I is formally most related to the porphyrins

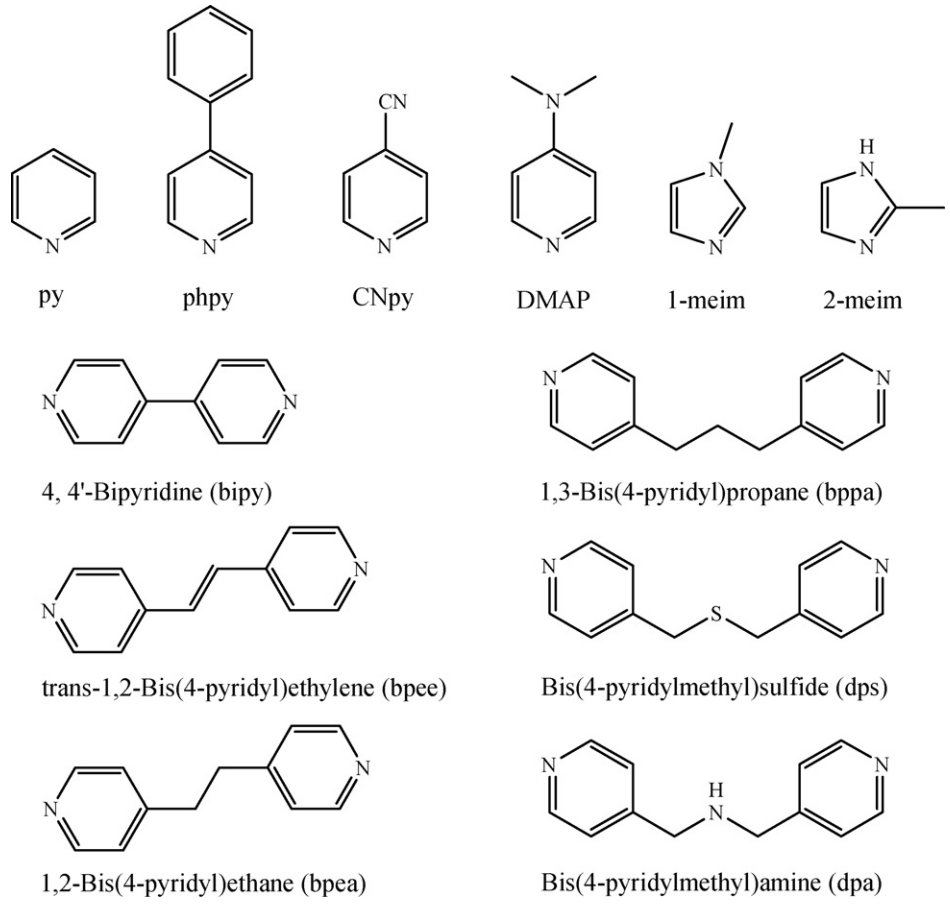

Scheme 2. Overview of the axial ligands, with their abbreviations, used in this work.

with a tetradentate macrocycle and a N_4^{2-} donor atom set. Indeed, the properties of these iron complexes are very similar to the porphyrins, but some special features can also be observed [11]. Type II are tetradentate open chain ligands with an $N_2O_2^{2-}$ coordination sphere. Iron(II) complexes of this ligand type with N-heterocycles as axial ligands are suitable for the synthesis of spin crossover complexes, whose properties are reviewed in this article. The general structure of the ligands (L1) and their derivatives (L2) used for the synthesis of dinuclear complexes is given in Scheme 1. An overview of the axial ligands used, is given in Scheme 2. Type III are tridentate ligands that promote the formation of oligonuclear structures [12] similar to those found in biological systems. Investigations on copper, cobalt and nickel complexes of the monomer ligands showed that the variation of the substituents $R^{1/2}$ can be used to control the properties of the metal center such as (i) the electronic state of the central atom [13], (ii) the redox potentials [14], (iii) the affinity of vacant axial coordination sites towards additional ligands [15] and (iv) the binding and activation of small molecules as dioxygen, carbon dioxide or nitric oxide [16]. This situation is particularly true for the chemistry of the iron complexes where marginal ligand variations can dramatically change the properties of the system [10,11,17].

3. The mononuclear building blocks

3.1. General trends

The general route for the synthesis of octahedral iron complexes is the conversion of the free equatorial ligands with iron(II)acetate and an excess of the axial ligand in a suitable solvent, mostly methanol (route 1). Alternatively, an iron complex of the tetradentate equatorial ligand with methanol as axial ligands, $[FeL1(MeOH)_2]$ can be prepared in a first step and this is then converted with the desired axial ligand in a second step (route 2). Both synthetic routes often give the same results, but not necessarily. A 1:2 ratio of equatorial:axial ligand results in the formation of pentacoordinate species. However, in some cases pentacoordinate complexes are obtained irrespective of the excess of axial ligand. In these cases, a variation of the solvent was necessary in order to obtain the six-coordinate species. The results of the different synthetic approaches and their magnetic properties are summarized in Table 1.

Table 2
Redox potentials $Fe^{II/III}$ of the iron(II) complexes (values E_{SCE} from Ref. [18] converted to E_H with $E_H = E_{SCE} + 0.24$ V) in pyridine or DMF and spin ground state of the corresponding nitrosyliron complexes [19].

Complex	Fe1a	Fe1b	Fe1c	Fe1d
*E*H(Py) [V]	0.42	0.38	0.46	>0.6
*E*H(DMF) [V]	0.25	0.24	0.27	0.41
S (nitrosyliron complex)	1/2	1/2 ⇔ 3/2	1/2 ⇔ 3/2	3/2

Two general trends can be deduced from this compilation: the more electron withdrawing substituents at the equatorial ligand stabilize the high-spin ground state of the complexes. The same can be said about the more basic axial ligands. In the case of the equatorial ligands, the ligand field strength increases in the order $d < c < a \approx b$. This correlates well with the redox potentials $Fe^{II/III}$ of the iron(II) complexes (values E_{SCE} from Ref. [18] converted to E_H with $E_H = E_{SCE} + 0.24$ V) in pyridine or DMF. The redox potentials are strongly influenced by the (−)-*I* character of the substituents; the stronger electron withdrawing substituents stabilize lower oxidation states. In contrast to this, the ligand field strength correlates with the (−)-*M* character of the substituents resulting in a reverse order. The results obtained are in good agreement with the spin ground state of a series of nitrosyliron complexes of the same ligand type [19] (Table 2).

The influence of the substituents a and b on the ligand field strength is very similar and the overall ligand field strength depends on the axial ligands used and, as most of the investigations are carried out in the solid state, on intermolecular interactions.

In Fig. 1 the $T_{1/2}$ ($\gamma_{HS} = 0.5$) values of the different SCO complexes are plotted against the pK_a values of the axial ligands used. If available, the data obtained from investigations in solution (see NMR spectroscopy) were included as well. When interpreting the results, one has to keep in mind that in the solid state $T_{1/2}$ is strongly influenced by intermolecular interactions, especially when abrupt spin transitions with hysteresis are obtained. This results in discrepancies between the $T_{1/2}$ values obtained from SQUID measurements and those obtained in solution. Additionally the pK_a values reflect only the σ-donor ability of the ligands ignoring the π-acceptability that is also important for the overall ligand field strength. The different values obtained for the complexes with pyridine and 4-phenylpyridine demonstrate this clearly. Nevertheless, a clear trend can be observed. Higher pK_a values that correspond to a better

Table 1
Overview of octahedral mononuclear iron(II) complexes and their magnetic properties discussed in this work.

	$[Fe1a(L_{ax})_2]$	$[Fe1b(L_{ax})_2]$	$[Fe1c(L_{ax})_2]$	$[Fe1d(L_{ax})_2]$
py	$[Fe1a(py)_2]$[a] $T_{1/2}$ = 220 K, gradual	$[Fe1b(py)_2]$[a] $T_{1/2}$ = 190 K, hysteresis 2 K	$[Fe1c(py)_2]$[a] HS	$[Fe1d(py)_2](py)$[a] HS
phpy	$[Fe1a(phpy)_2]$[a] $T_{1/2}$ = 234 K, hysteresis 4 K	$[Fe1b(phpy)_2](phpy)$[a] $T_{1/2} \approx 290$ K, gradual	–	–
CNpy	$[Fe1a(CNpy)_2](CNpy)_{0.25}$[c] $T_{1/2}$ = 265 K, 114 K, step-wise	$[Fe1b(4\text{-}CNpy)_2]$[b] $T_{1/2} \approx 340$ K, gradual	$[Fe1c(CNpy)_2]$[b] HS	–
DMAP	$[Fe1a(DMAP)_2]$[c] HS	$[Fe1b(DMAP)_2]$[c] $T_{1/2}$ = 179 K, hysteresis 9 K	$[Fe1c(DMAP)_2]$[c] HS	$[Fe1d(DMAP)_2]$[c] HS
1-meim	$[Fe1a(1\text{-}meim)_2]$[b] HS	$[Fe1b(1\text{-}meim)_2](1\text{-}meim)$[b,d] $T_{1/2}$ = 178 K, hysteresis 2 K $[Fe1b(1\text{-}meim)_2]$[c] $T_{1/2}$ = 179 K, abrupt $[Fe1b(1\text{-}meim)_2](DMF)$[a,e] $T_{1/2} \approx 80$ K, incomplete	$[Fe1c(1\text{-}meim)_2]$ HS	$[Fe1d(1\text{-}meim)_2]$ HS
2-meim	$[Fe1a(2\text{-}meim)_2]$ HS	–	–	–

[a] Route 1 used for the synthesis.
[b] Route 2 used for synthesis.
[c] Both routes lead to the same result.
[d] 1-meim as solvent.
[e] DMF as solvent.

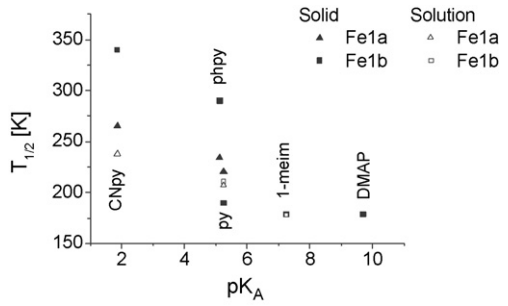

Fig. 1. Plot of $T_{1/2}$ of the mononuclear complexes against the pK_a values of the axial ligands used.

σ-donor ability of the ligand, stabilize the HS state resulting in a decrease of $T_{1/2}$.

Results from X-ray structure analysis are available for 13 of the 20 complexes. Selected bond lengths and angles are summarized in Table 3. Intramolecular changes during the spin transition: the average bond lengths within the first coordination sphere in the high-spin state are 2.08 Å (Fe–N_{eq}), 2.02 Å (Fe–O_{eq}) and 2.25 Å (Fe–N_{ax}). Upon spin transition a shortening of the bond lengths of about 10%, as discussed for other iron(II) spin crossover complexes in literature [1], is observed. This shortening is more pronounced for the axial than for the equatorial ligands. The average distances in the low-spin state are 1.91 Å (Fe–N_{eq}), 1.95 Å (Fe–O_{eq}) and 2.01 Å (Fe–N_{ax}). A second sensible tool for determining the spin state of these types of iron complexes is the O–Fe–O angle, the so-called bite of the ligand. It changes from an average of 108° in the high-spin state to 90° in the low-spin state. In Fig. 2 a top view of the molecule structure of [Fe1b$(py)_2$], as a typical example in the high-spin and the low-spin form, is given together with the results from the magnetic measurements to illustrate the changes [21].

The bond lengths of the pure HS complexes are systematically longer than those of the SCO complexes in the HS state, but only for the equatorial ligand. The average values are 2.11 Å (Fe–N_{eq}), 2.05 Å (Fe–O_{eq}) and 2.24 Å (Fe–N_{ax}) for the pure HS complexes and 2.07 Å (Fe–N_{eq}), 2.00 Å (Fe–O_{eq}) and 2.25 Å (Fe–N_{ax}) for the spin crossover compounds. The average O–Fe–O angle also varies from 112° for the pure HS compounds to 107° for the SCO systems. One possible explanation is that the X-ray structures of the HS form were determined at too low temperatures with a small fraction of the molecules in the crystal already in the LS state and therefore shorter average bond lengths are observed. Then, however, the distance to the axial ligand would also show this effect, which is not the case. The second possibility is that due to packing effects (intramolecular interactions, steric hindrance) for some of the pure HS compounds, longer distances are observed. As the ligand field

Table 3
Selected bond lengths [Å] and angles [°] within the first coordination sphere of octahedral mononuclear iron(II) complexes with the spin state *S*.

Complex	*T* [K]	*S*	Fe–N_{eq}	Fe–O_{eq}	Fe–N_{ax}	O1–Fe–O2	N_{ax}–Fe–N_{ax}	∠ L1, L2[c]	Ref.
[Fe1a$(py)_2$]		2	2.062(4)	2.017(4)	2.256(5)	106.3(1)			[20]
			2.053(4)	1.990(3)	2.195(4)				
		0	1.923(3)	1.962(2)	2.025(3)	92.4(1)			
			1.918(2)	1.955(2)	2.023(3)				
[Fe1b$(py)_2$]	200	2	2.061(2)	1.992(1)	2.226(2)	106.99(5)	175.6(1)	16.7	[21]
			2.074(1)	2.009(1)	2.269(2)				
	150	0	1.894(1)	1.930(1)	2.007(2)	89.98(5)	176.1(1)	15.4	
			1.906(1)	1.948(1)	2.025(2)				
[Fe1c$(py)_2$]		2	2.109(2)	2.046(1)	2.239(2)	112.04(6)		43.4	
			2.102(2)	2.048(1)	2.262(2)				
[Fe1d$(py)_2$](py)		2	2.100(4)	2.083(4)	2.262(5)	108.0(2)		53.9	[22]
			2.141(6)	2.050(4)	2.246(4)				
[Fe1a$(phpy)_2$]	300	2	2.078(2)	2.000(2)	2.229(3)	107.25(8)	174.47(9)	61.3	[23]
			2.081(3)	2.009(2)	2.289(3)				
	130	0	1.921(4)	1.952(3)	1.989(4)	89.5(1)	174.7(1)	73.6	
			1.922(3)	1.967(3)	2.009(3)				
[Fe1b$(phpy)_2$](phpy)	125	0	1.902(2)	1.950(2)	2.013(3)	89.11(8)	174.84(9)	81.1	[23]
			1.910(2)	1.952(2)	2.015(3)				
[Fe1a$(DMAP)_2$]	293	2	2.082(4)	2.017(3)	2.220(4)	111.2(1)	169.1(2)	16.2	[24]
			2.097(4)	2.018(3)	2.304(4)				
[Fe1b$(DMAP)_2$]	293	2	2.085(4)	2.008(3)	2.231(4)	109.1(2)	171.4(2)	74.6	[21]
			2.090(4)	2.025(3)	2.272(5)				
[Fe1a$(CNpy)_2$]$(CNpy)_{0.25}$	100	0, 0	1.895(2)	1.942(2)	1.979(2)	90.23(6)	174.7(1)	80.1	[25]
			1.899(2)	1.947(2)	1.985(2)				
			1.899(2)	1.933(2)	2.008(2)	89.89(6)	176.1(1)	7.7	
			1.909(2)	1.938(2)	2.009(2)				
	240	2, 0	1.911(2)	1.944(1)	1.999(2)	91.70(5)	174.4(1)	80.3	
			1.911(2)	1.951(1)	2.007(2)				
			2.034(2)	1.967(2)	2.228(2)	102.74(6)	175.9(1)	6.6; 77.3	
			2.040(2)	1.973(2)	2.231(2)				
	293	2, 2	2.061(2)	1.978(1)	2.289(2)	105.39(6)	176.1(1)	77.6	
			2.068(2)	1.982(1)	2.285(2)				
			2.029(2)	1.970(1)	2.177(2)	103.61(6)	173.8(1)	7.7	
			2.037(2)	1.992(1)	2.238(2)				
[Fe1a$(1\text{-meim})_2$]	200	2	2.113(2)	2.050(2)	2.204(2)	115.36(7)	172.4(1)	7.1	[26]
			2.125(2)	2.080(2)	2.211(2)				
[Fe1b$(1\text{-meim})_2$](1-meim)	250	2	2.083(2) 2.077(2)	1.999(2) 2.009(2)	2.250(3) 2.279(3)	106.84(7)	179.24(8)	59.6	[27]
	135	0	1.892(3) 1.899(3)	1.934(2) 1.940(2)	2.012(3) 2.016(3)	88.36(9)	178.97(11)	56.5	
[Fe1b$(1\text{-meim})_2$](DMF)	125	2	2.089(2)	2.008(2)	2.259(2)	107.59(6)	177.3(1)	57.1	[26]
			2.108(2)	2.034(2)	2.302(2)				
[FeL1a$(2\text{-meim})_2$]	200	2	2.113(2)	2.040(2)	2.235(2)	113.99(6)	164.93(7)	86.9	[26]
			2.113(2)	2.059(2)	2.239(2)				

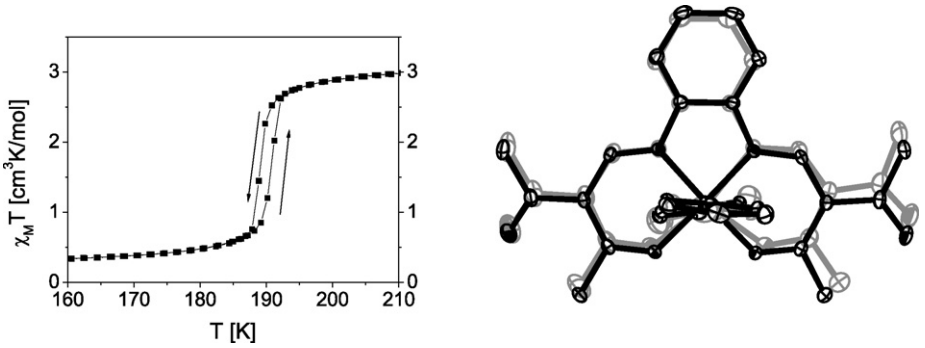

Fig. 2. Thermal dependence of $\chi_M T$ (left) and schematic drawing of the top view of both HS and LS forms of [Fe1b(py)$_2$] (right). The asymmetric unit at $T \cong 150$ K is the upper one. Fe–N_{eq} bonds are superimposed. The change in the O–Fe–O angle (HS: 107°, LS: 90°) is clearly visible [21].

strength strongly depends on those distances this might be the reason why the compounds crystallize as HS complexes. Investigation in solution is necessary to see if this is indeed the case.

The conformation of the axial ligands is independent of the equatorial and axial ligands used and does not change significantly during the spin transition in all cases. For most of the complexes weak intramolecular hydrogen bonds between the C–H hydrogen of the aromatic pyridine or imidazole ring of the axial ligand and the coordinated N or O of the equatorial ligand are observed. Those interactions are most likely the main factor that determines the orientation of the axial ligands.

3.2. Influence of different molecules on the crystal packing

The combination of the equatorial ligand L1b and 1-meim as axial ligand is a good example to demonstrate the different products obtained for different synthetic approaches. A direct conversion of the equatorial ligand with iron acetate in methanol in the presence of the axial ligand always led to the pentacoordinate species irrespectively of the ratio used [26]. If the solvent is changed and the conversion is performed in pure 1-meim or in DMF, a six-coordinate compound is obtained with one additional solvent molecule per iron center in the crystal [26,27]. Finally, if the strategy is changed and the iron complex [Fe1b(MeOH)$_2$] is used as the starting material in a methanol/1-meim mixture, a six-coordinate powder sample with no additional solvent molecules is obtained [26]. The inclusion of DMF significantly lowers the transition temperature from 179 K to approximately 80 K. The reason for this significant influence is the existence of weak (or non-classical) hydrogen bonds between the DMF oxygen and one of the aromatic hydrogen atoms of the axial 1-meim. These interactions lead to an increase of the Fe–L_{ax} distance and hence lower the transition temperature. In the powder sample [Fe1b(1-meim)$_2$] and the crystalline charge [Fe1b(1-meim)$_2$](1-meim), nearly the same transition temperatures are observed but with different degrees of cooperative interactions. They lead to a small hysteresis for the crystalline charge and an abrupt transition in the powder sample—a behavior that can easily be explained with the domain model if smaller domains are assumed for the powder sample.

A second example demonstrating the influence of the inclusion of additional ligand molecules is the complex [Fe1a(CNpy)$_2$](CNpy)$_{0.25}$, where a step-wise spin transition with a wide plateau in the region of 125–225 K is observed (Fig. 3) [25]. In contrast to other step-wise spin crossover compounds, the plateau at $\gamma_{HS} = 0.25$ cannot be directly correlated to the number of inequivalent iron sites in the asymmetric unit. The reason for the significantly lower transition temperature of one fourth of the iron centers is an additional distorted 4-CNpyridine molecule in the crystal packing that has a noticeable short Fe–N distance to a quarter of the complex molecules. This observation is supported by Mössbauer spectroscopy. Here, the line width of the LS doublet at 80 K is wider than expected and the doublet is asymmetric—two indications for two or more unequivalent iron sites. In the region of the plateau, the line widths are smaller—one of the two iron sites is still in the LS state and the other one is in the HS state (Fig. 4). Around 240 K ($\gamma_{HS} = 0.5$) an inflection point is observed in the magnetic measurements where the characteristic of the spin transition changes from gradual to abrupt with small hysteresis. This behavior can be explained by the cooperative interactions among the phenylene rings of neighboring molecules (π-stacking). The coexistence of two different effects that influence the transition temperature (distorted additional 4-cyanopyridine) as well as the cooperative

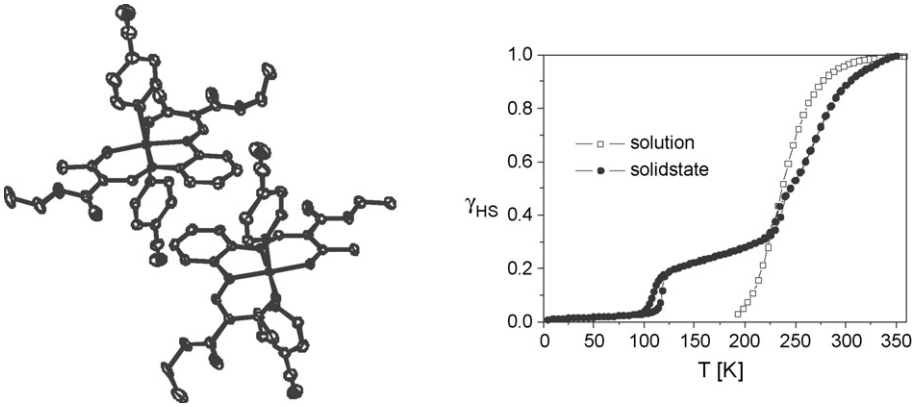

Fig. 3. . Thermal dependence of $\chi_M T$ (right) and ORTEP drawing of the asymmetric unit of [Fe1a(CNpy)$_2$](CNpy)$_{0.25}$ at 240 K (left). Hydrogen atoms and solvent molecules were omitted for clarity. Thermal ellipsoids are shown at the 50% probability level [25].

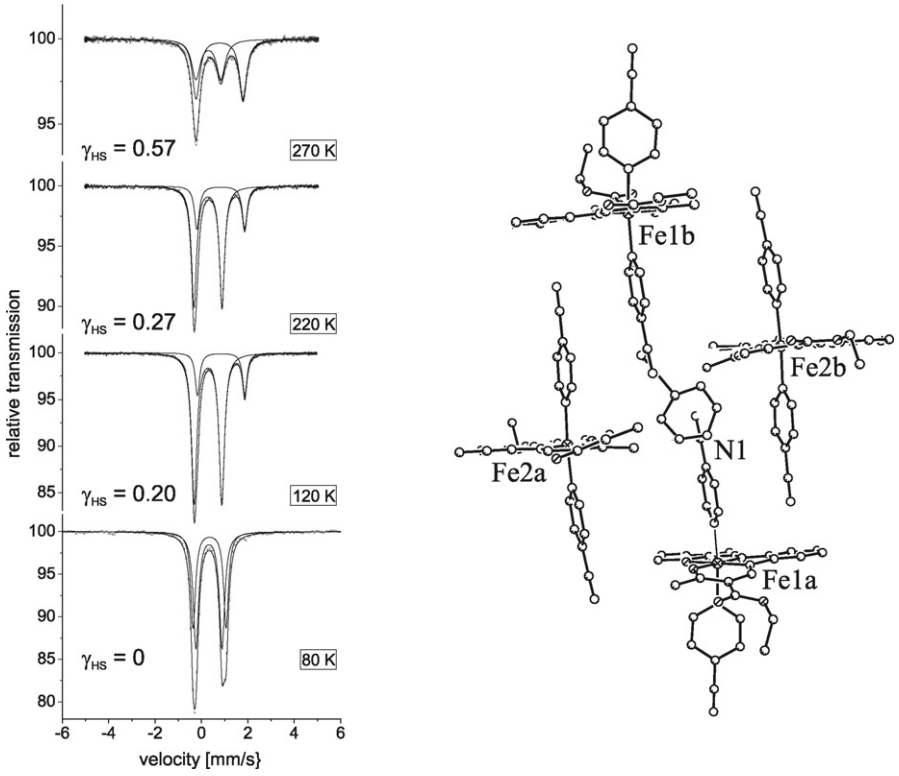

Fig. 4. Plot of the Mössbauer spectra of $[Fe1a(CNpy)_2](CNpy)_{0.25}$ at 80, 120, 220 and 270 K with the high-spin molar fraction indicated (left) and packing of the molecules in the crystal around the CNpy molecule at 100 K [25].

interactions during the spin transition (π-stacking) are responsible for the complex structure of the transition curve. In solution a gradual spin transition with $T_{1/2}$ close to the first step in the transition curve of the solid sample is observed (Fig. 3) [25].

3.3. Understanding cooperative interactions

For the mononuclear complexes summarized in Table 1, different degrees of cooperative interactions are observed. The properties of the spin transition curve range from gradual (e.g. $[Fe1a(py)_2]$) to abrupt with hysteresis (e.g. $[Fe1b(DMAP)_2]$). The only possible reason for the cooperative interactions is short van der Waals contacts between the neighboring molecules for all examples. The extent of the cooperative interactions must therefore correlate with the number of short contacts and the dimension of the built network. The available structures were therefore analyzed with respect to this and the results are summarized in Table 4. Following the suggestion of Purcell et al. [28] the parameter C ($=\Gamma/2RT_{1/2}$ = cooperativity factor; with Γ the intermolecular interaction parameter) was determined for all complexes to allow a better comparison of the extent of the cooperative interactions. To give an estimation of the molecule size the diameters a and b defined according to Ref. [23] are given as well.

At first glance, no clear correlation is visible from the compilation in Table 4. Complexes with gradual spin transition ($[Fe1a(py)_2]$) show a similar number of short contacts as complexes with small hysteresis ($[Fe1b(py)_2]$). The complex with the widest hysteresis ($[Fe1b(DMAP)_2]$, 9 K) does not have the highest number of short intermolecular contacts, but, in the literature the extent of cooperative interactions is always correlated with the number of contacts [8j]. The reason for these discrepancies is the varying effectiveness of the contacts for the transmission of elastic interactions. For complexes of the equatorial ligand L1a, the intermolecular interactions are often mediated through the rather flexible ethoxy group of the substituents. The pair $[Fe1a(py)_2]$ and $[Fe1b(py)_2]$ illustrates rather nicely that those interactions can have little-to-no relevance. Rigid and sterically demanding axial ligands such as 4-phenylpyridine are necessary to obtain relevant enough contacts. Similar conclusions are obtained if the size of the molecule is considered. The substituents of L1a increase the size of the molecule compared to

Table 4
Overview of the intermolecular interactions between the mononuclear octahedral iron(II) complexes with the cooperativity parameter C indicated and the diameters a and b.

Complex	$T_{1/2}$ [K]	C	Number of short contacts (HS/LS)[a]	Dimension	a[b] (HS/LS) [Å]	b[c] (HS/LS) [Å]
$[Fe1a(py)_2]$	220	0	3/5	2D layer	11.9/11.6	16.2/16.0
$[Fe1a(phpy)_2]$	234	1.03	6/8	3D network	20.5/20.1	16.1/16.3
$[Fe1b(py)_2]$	190	1.08	3/4	2D layer	11.9/11.5	12.9/12.8
$[Fe1b(phpy)_2](phpy)$	290	0	–/3	1D chain	–/20.1	–/12.8
$[Fe1b(DMAP)_2]$	179	1.28	6/–	3D network	16.1/–	12.9/–
$[Fe1b(1\text{-}meim)_2](1\text{-}meim)$	178	1.11	3/4	2D layer	12.6/12.1	12.8/12.8

[a] Contacts shorter than the sum of the van der Waals radii −0.1 Å are considered.
[b] Longest distance between the axial ligands.
[c] Longest distance within the equatorial ligand.

the substituents of L1b. It can easily be imagined that for larger molecules (or more simple larger spheres) more contacts are necessary to effectively transmit the geometric changes occurring during the spin transition through the crystal. If those two points are considered, the effectiveness of the contacts if flexible groups are considered and the number of contacts in relation to the molecule size, all the predictions made in literature for other systems [8i] also work for our complexes and the strength of the cooperative interactions correlate well with the number of the intermolecular contacts.

3.4. Photomagnetic properties

The photomagnetic properties of 5 of the 9 SCO complexes with complete spin transition were investigated, namely [Fe1a(phpy)2] [23], [Fe1a$(CNpy)_2$]$(CNpy)_{0.25}$ [25], [Fe1b$(py)_2$] [21], [Fe1b$(phpy)_2$](phpy) [23] and [Fe1b$(DMAP)_2$] [21]. For those investigations, the first step is always to record the temperature dependence of the reflectivity spectra of the compounds. Due to the dark color of the complexes, the signal is always close to saturation. Nevertheless it was possible to follow the thermal spin transition in all cases. A decrease of the absorption band around 800—850 nm, which is a characteristic of the d–d transition of the HS state, can be observed. For four of the five complexes (all except [Fe1b$(phpy)_2$](phpy)) the reflectivity signal of this transition band increases again at temperatures below 50 K. This is an indication of a photoinduced switching into the HS state at low temperatures (LIESST-effect, with LIESST = light-induced excited spin state trapping) and consequently the photomagnetic properties of the three most promising complexes were investigated using a SQUID magnetometer. Due to the dark color only low levels of photoexcitation could be obtained using the bulk material. The highest level obtained is 60% for [Fe1b$(DMAP)_2$] [21]. In Fig. 5 the results from the photomagnetic investigations for this complex are summarized.

The T(LIESST) temperature of the complexes, above which the light-induced magnetic HS information is erased in a SQUID cavity [29], is comparatively low. According to the inverse energy gap law introduced by Hauser [30] or the T(LIESST) versus $T_{1/2}$ relation of Létard and co-workers [29,31] the T(LIESST) temperature depends inversely on $T_{1/2}$ and additionally on the rigidity of the inner coordination sphere around the iron center. The weak stabilization of the photoinduced HS state for these types of complexes can be attributed to the flexibility of the tetradentate ligand around the unsaturated nitrogen atoms connecting the aromatic phenyl rings. The T(LIESST) values of the complexes under investigation is more in the region expected for complexes with monodentate or bidentate ligands.

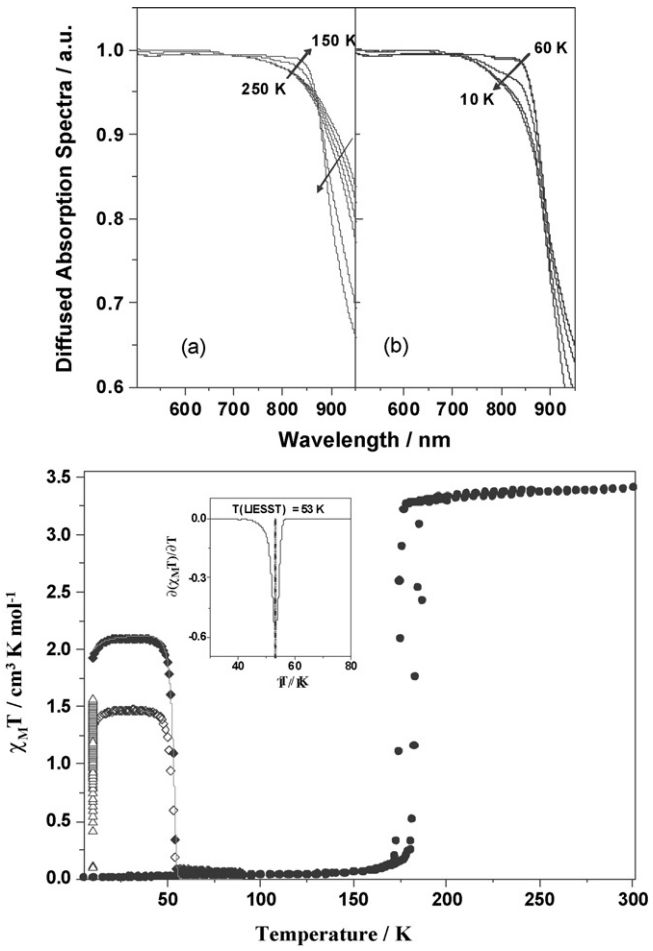

Fig. 5. Top: The dependency of the diffuse absorption spectra of [Fe1b$(DMAP)_2$] as a function of both temperature and light irradiation with (a) the thermal spin crossover and (b) the light-induced regions. Bottom: Temperature dependence of $\chi_M T$ for [Fe1b$(DMAP)_2$]. (●) Data recorded in the cooling and warming mode without irradiation; (△) data recorded with irradiation at 10 K; (♦) T(LIESST) measurement, data recorded in the warming mode with the laser turned off after irradiation for 1 h at 752.5–799.3 nm ((◊) at 647.1–676.4 nm). The solid line through the T(LIESST) measurement shows the fit generated from the deduced experimental thermodynamic parameters. The insert figure reports the region where the minimum of the derivate d$\chi_M T$/dT curve gave the T(LIESST) temperature. Reprinted with permission from Ref. [21]. Copyright 2007 The American Chemical Society.

4. From monomer to polymer systems

The reason for the step to go from monomer to polymer systems has been given in the introduction and the results for the mononuclear complexes demonstrate again the importance of the intermolecular interactions for cooperative spin transitions and the difficulties encountered controlling those interactions. The ligand system used is very well suited for the synthesis of 1D polymer chain compounds. One simply has to replace the monodentate axial ligand used so far by a bidentate bridging ligand, and a polymer chain is obtained. Pure products are only obtained if the iron(II) complex of the equatorial ligand with monodentate axial ligands (mostly methanol, but not necessarily) is used as starting material. A one-pot reaction of iron(II) acetate with the desired equatorial and axial ligands as frequently used for the monomer species often leads to the formation of product mixtures. However, the synthetic strategy has one great benefit, namely the suitability to use this synthetic approach for diffusion-controlled crystallization setups. Thus we were able to obtain X-ray structures for 6 of the 19 synthesized polymer complexes. In Table 5 the properties of the different polymer chain compounds synthesized so far are summarized and in Table 6 selected bond lengths and angles of the structurally characterized complexes are given.

The bond lengths and angles within the first coordination sphere of the iron center are in the same region as observed for the mononuclear complexes. The average values are 2.08 Å (Fe–N_{eq}), 2.01 Å (Fe–O_{eq}) and 2.26 Å (Fe–N_{ax}) in the HS state and 1.92 Å (Fe–N_{eq}), 1.95 Å (Fe–O_{eq}) and 2.02 Å (Fe–N_{ax}) in the LS state. Again, the bite of the equatorial ligand is a suitable tool to determine the spin state of the iron center from X-ray structure analysis. It changes from 110° in the HS state to 92° in the LS state.

4.1. Increasing cooperative interactions

The first polymer SCO complex synthesized of this ligand type was the compound [Fe1b(bipy)] [32]. An excerpt of the 1D chain

Table 5
Overview of octahedral iron(II) coordination polymers discussed in this work and their magnetic properties.

	[Fe1a(L_{ax})]	[Fe1b(L_{ax})]	[Fe1c(L_{ax})]
bipy	[Fe1a(bipy)]	[Fe1b(bipy)]	–
	HS	$T_{1/2}$ = 228 K, hysteresis 18 K	
		[Fe1b(bipy)](MeOH)$_{0.25}$	
		HS	
		[Fe1b(bipy)](DMF)	
		HS	
bpea	[Fe1a(bpea)]	[Fe1b(bpea)]	–
	$T_{1/2}$ = 190 K, gradual, incomplete	$T_{1/2}$ = 123 K, 95 K, hysteresis 11 K, 9 K, step-wise	
		[Fe1b(bpea)](MeOH)$_{0.5}$	
		$T_{1/2}$ = 106 K, 98 K, hysteresis 22 K, 7 K, step-wise	
bpee	[Fe1a(bpee)]	[Fe1b(bpee)]	–
	HS	HS	
bppa	[Fe1a(bppa)]	[Fe1b(bppa)](MeOH)	[Fe1c(bppa)]
	$T_{1/2} \approx$ 200 K, gradual, incomplete	$T_{1/2}$ = 166 K, 90 K, step-wise	HS
		[Fe1b(bppa)](EtOH)	
		$T_{1/2}$ = 117 K, incomplete	
dpa	[Fe1a(dpa)]	[Fe1b(dpa)]	–
	$T_{1/2}$ = 175 K, hysteresis 4 K, incomplete	HS	
dps	[Fe1a(dps)]	[Fe1b(dps)](MeOH)	–
	$T_{1/2}$ = 197 K, gradual, incomplete	HS	
	[Fe1a(dps)]	[Fe1b(dps)](EtOH)	
	$T_{1/2}$ = 172 K, abrupt	$T_{1/2}$ = 85 K, gradual, incomplete	

Table 6
Selected bond lengths [Å] and angles [°] within the first coordination sphere of octahedral polymer iron(II) complexes with the spin state *S*.

	T [K]	*S*	Fe–N_{eq}	Fe–O_{eq}	Fe–N_{ax}	O1–Fe–O_2	N_{ax}–Fe–N_{ax}	Ref.
[Fe1b(bipy)] (MeOH)$_{0.25}$	250	2	2.06	1.99	2.24	113	174	[32]
[Fe1b(bipy)] (DMF)	200	2	2.090(3), 2.087(4)	2.016(3), 2.010(3)	2.301(3), 2.274(3)	108.13(12)	176.99(13)	[24]
[Fe1b(bpea)] (MeOH)$_{0.5}$	200	2	2.086(2), 2.086(2)	2.004(2), 2.019(2)	2.252(2), 2.284(2)	109.54(6)	176.92(7)	[33]
[Fe1a(bpee)] (MeOH)	200	2	2.101(5), 2.092(5)	2.044(4), 2.017(4)	2.262(4), 2.280(4)	112.71(17)	169.76(17)	[24]
[Fe1b(bppa)] (MeOH)	225	2	2.081(2), 2.097(2)	2.010(2), 2.013(2)	2.266(2), 2.238(2)	109.71 (6)	173.38 (7)	[33]
	125	2	2.066(3), 2.074(3)	2.004(2), 2.009(2)	2.223(3), 2.237(3)	107.65 (10)	172.60 (12)	
		0	1.910(3), 1.920(3)	1.946(3), 1.947(2)	1.997(3), 2.034(3)	92.06 (10)	174.57 (12)	
[Fe1b(dpa)] (EtOH)	200	2	2.102(2), 2.095(2)	2.033(2), 2.028(2)	2.250(3), 2.252(3)	110.37(8)	169.45(9)	[24]

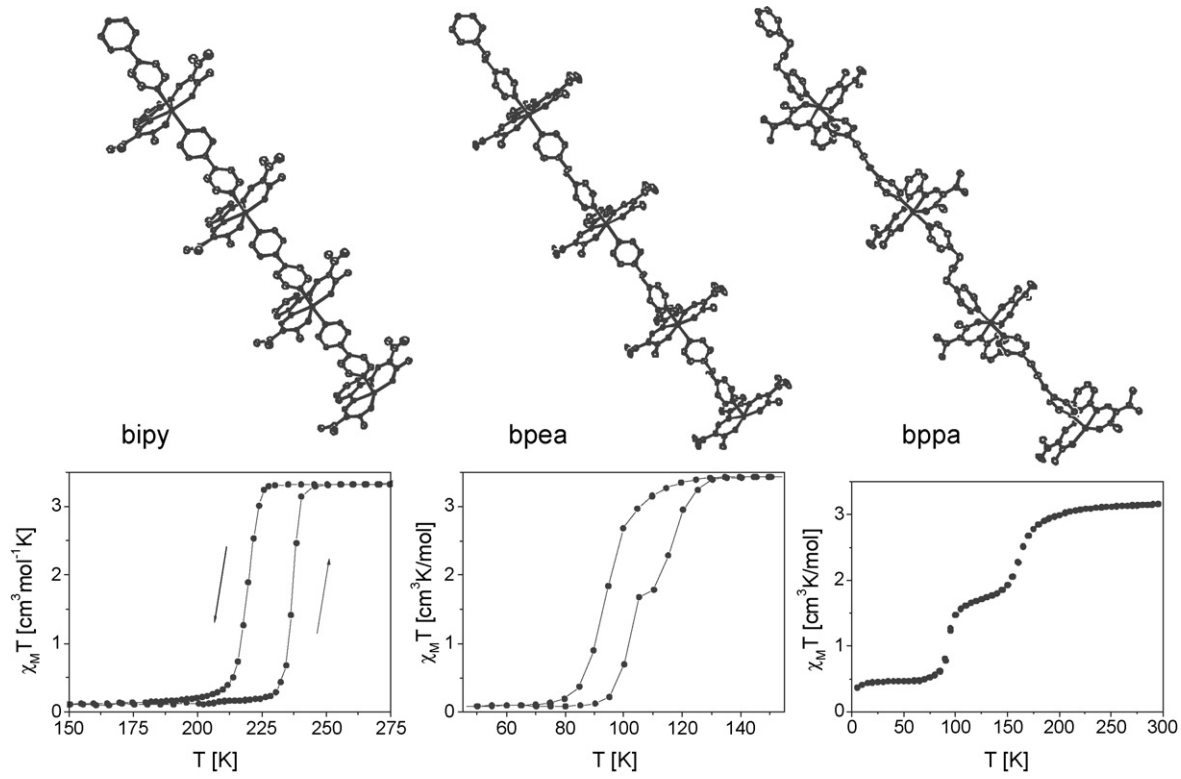

Fig. 6. . X-ray structure (top) and magnetic properties (bottom) of the three 1D chain compounds [Fe1b(bipy)] [32a], [Fe1b(bpea)](MeOH)$_{0.5}$ and [Fe1b(bppa)](MeOH) (from left to right, respectively).

structure and the observed magnetic properties of the powder sample are given in Fig. 6, left hand side. A linear chain of linked iron centers is observed and the magnetic measurements reveal an abrupt spin transition with 18 K wide thermal hysteresis loop [32a]. Comparison of the results with those of the mononuclear analog, [Fe1b(py)$_2$], given in Fig. 2 and Table 1, the hysteresis width increases significantly (from 2 to 18 K) when going from the monomer to the polymer system and the synthetic strategy appears to work.

For the propagation of the volume changes during the spin transitions, the focus is set on rigid linkers. Indeed, the introduction of ethyl or propyl groups in the covalent bipyridine bridge (Fig. 6, middle and right hand side) decreases the cooperative interactions and for the very flexible bppa ligand, only abrupt spin transitions are observed. Despite these very promising results, the number of coordination polymers showing spin transition with thermal hysteresis loop is still limited [8i]. Indeed, the widest thermal hysteresis loops are associated with π-stacking interactions between monomer complexes [34]. In the case of 4,4′-bipyridine linked iron(II) chain compounds, other examples with structural motives that are very similar to compound [Fe1b(bipy)] are reported in literature. One example is the complex [Fe(aqin)$_2$(bipy)](ClO$_4$)$_2$ 2EtOH (aqin = 8-amino-quinoline) [8a]. Its molecule structure and magnetic properties are given in Fig. 7. Despite the very similar structural motive; the bond lengths around the bipy ligand and the Fe···Fe distances within the polymer chain are essentially the same (Fe···Fe: both 11.5 Å [32a,8a]); for this complex only a gradual spin transition is observed. This leads to the question about the influence of the covalent bipy bridge on the cooperative interactions. An answer can be obtained if the packing of the molecules in the crystal, given in Fig. 8 for both complexes, is compared. For compound [Fe1b(bipy)] several short contacts between neighboring molecules can be observed, resulting in a 3D network of linked molecules while for [Fe(aqin)$_2$(bipy)](ClO$_4$)$_2$ 2EtOH no direct contacts are observed and all the bridging interactions (hydrogen bonds) are mediated over the counter-ion ClO$_4^-$. Similar to the observations made for the mononuclear complexes, the packing of the molecules in the crystal is the main factor determining the magnetic properties. The composition of the single crystals and the powder sample of [Fe1b(bipy)] is not exactly the same and therefore the magnetic properties differ, as discussed in the following section. However, as the powder sample can be prepared from the single crystals one may rest assured that the linear chain structure is the same in both samples. The differences in the magnetic properties are one further argument that interaction between the single chains is the main factor determining the SCO properties.

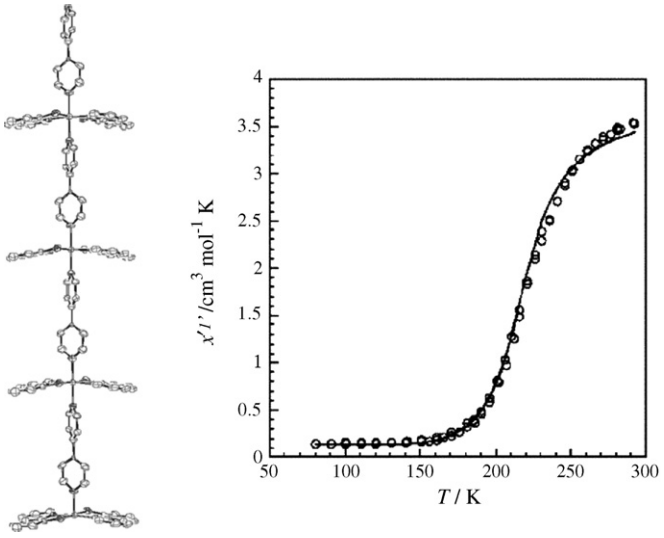

Fig. 7. X-ray structure (left) and magnetic properties (right) of the complex [Fe(aqin)$_2$(bipy)](ClO$_4$)$_2$ 2EtOH, Ref. [8a]. Reproduced by permission of the Royal Society of Chemistry on behalf of the Centre National de la Recherche Scientifique.

4.2. Effects of solvent molecules on the SCO behavior

Several attempts were made to determine the HS and LS structure of the polymer [Fe5b(bipy)] but they were not successful. However, in this case this was not due to a crumbling of the crystals during the phase transition as is sometimes observed for the mononuclear complexes, but due to the fact that the crystals remain in the HS state down to 20 K as illustrated in Fig. 9 [32]. Upon grinding, the SCO behavior of the powder sample reappears. Those grinding properties were highly unusual and completely contradictory to the observations made so far, where successive grinding leads to the disappearance of the hysteresis loop [35]. In order to understand this phenomenon, the different samples of [Fe5b(bipy)] were investigated in detail using magnetic measurements, optical reflectivity measurements and X-ray powder diffraction [32b]. The final result of the investigations was that the composition of the single crystals and the powder sample is slightly different and in the crystalline sample one quarter of a methanol molecule (solvent) per iron center is included in the crystal packing. This small difference drastically changes the magnetic properties of the complex, although the methanol is only very weakly bonded and easily lost in the grinding process or upon the heating of the sample [32b].

The strong dependence of the magnetic properties on solvent inclusion or exclusion is found for most of the other coordination polymers as well, as summarized in Table 4. In the case of [Fe1a(dps)], two different modifications with the same composition were obtained, depending on the solvent used for the synthesis of the complex (methanol or ethanol). Unfortunately, results from X-ray structure analysis are not yet available and the reason for the different magnetic properties is still unclear.

4.3. Two-step versus single step spin transitions

For the polymer SCO complexes under investigation frequently two-step or incomplete spin transitions are obtained as illustrated in Fig. 6 or summarized in Table 4. Different reasons for steps in the transition curve are discussed in literature. The first possibility—two or more non-equivalent iron centers [36] as observed for the mononuclear complex [Fe1a(CNpy)$_2$](CNpy)$_{0.25}$ [25], can be ruled out for the polymer systems as only one iron center per asymmetric unit is found for the structurally characterized examples. The second possibility is the formation of [HS–LS] spin-pair states as discussed for two-step spin transitions of dinuclear complexes [9,37]. Here weak antiferromagnetic interactions mediated over the bridging ligand are thought to be the reason for the occurrence of those mixed spin-pairs states [38]. This is not very likely for the systems presented here, as the bridging ligands are too extended to be seriously considered for the propagation of magnetic exchange interactions. Additionally, magnetic measurements on pure HS complexes of this ligand type demonstrated that there is no indication for magnetic exchange interactions [24]. Finally, there are two examples for mononuclear complexes with a unique crystallographic iron(II) site where some kind of antiferromagnetic interactions between the HS and the LS sublattices are made responsible for steps in the transition curve [3b,39]. For the complex [Fe1b(bppa)](MeOH) it was possible to determine the X-ray structure of the pure HS state and the mixed HS/LS state [33]. The complex crystallizes in the space group *C*2/*c* and at 225 K the asymmetric unit consists of one iron center that is clearly in the

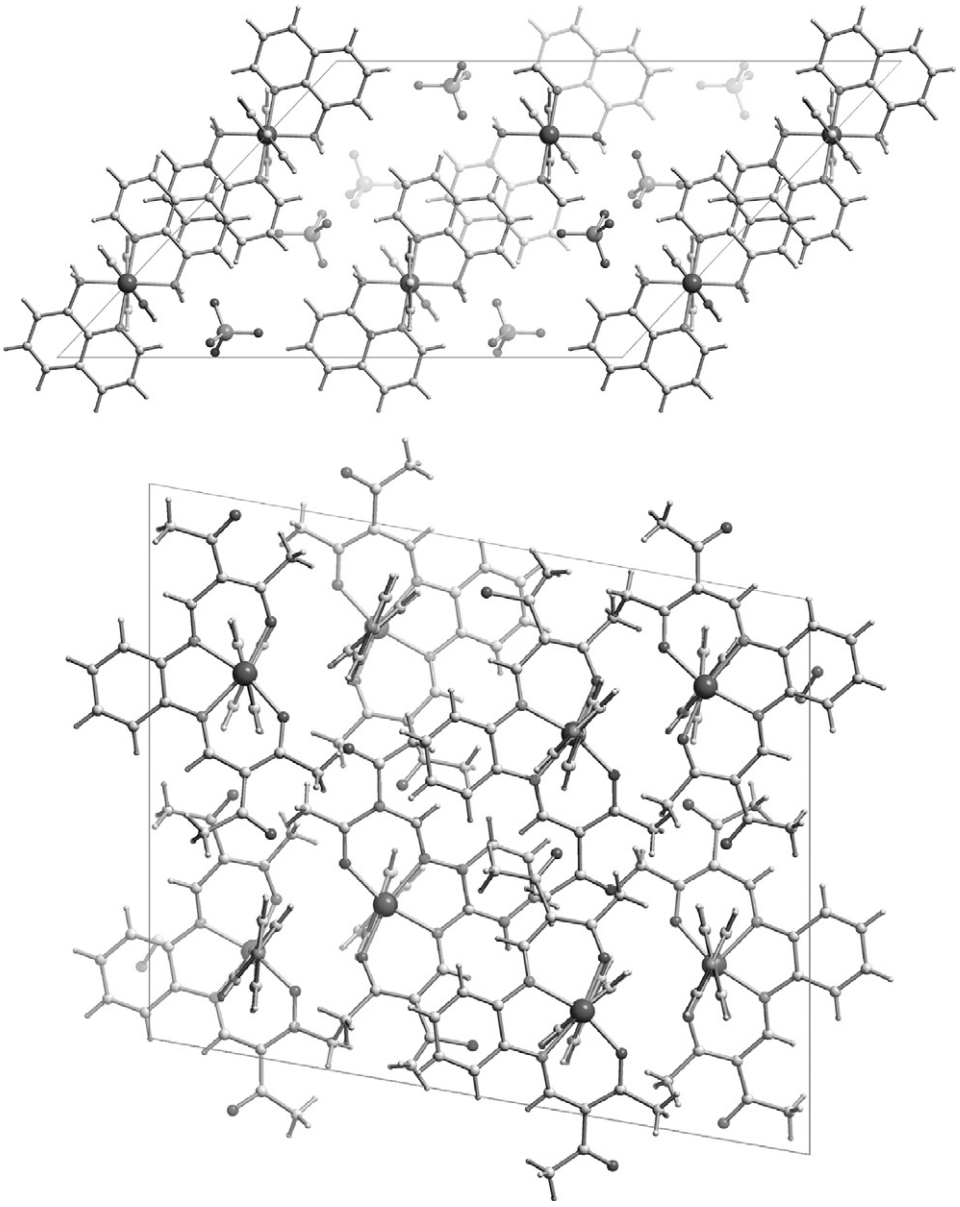

Fig. 8. Top view of the packing of the molecules in the crystal. Top: $[Fe(aqin)_2(bipy)](ClO_4)_2$ 2EtOH, Ref. [8a]. Reproduced by permission of the Royal Society of Chemistry on behalf of the Centre National de la Recherche Scientifique. Bottom: [Fe1b(bipy)] [32].

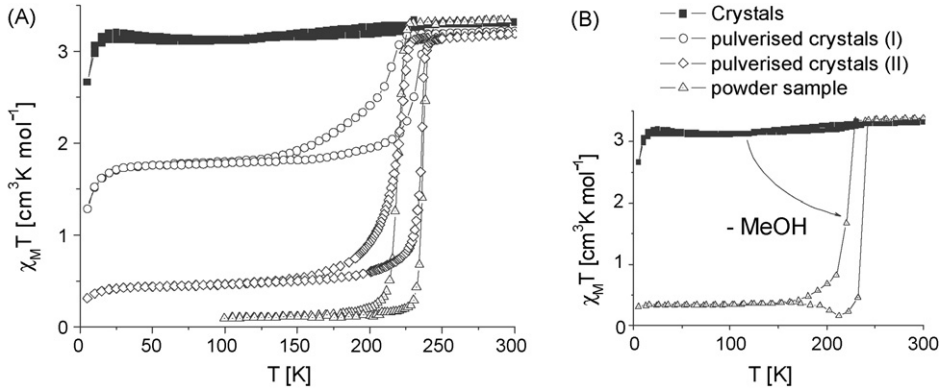

Fig. 9. Thermal variation of $\chi_M T$ for the different samples of [Fe1b(bipy)]. (A) Magnetic properties of the crystals $[Fe1b(bipy)](MeOH)_{0.25}$ (solid squares), pulverised crystals (open circles and open squares) and a separately prepared powder sample [Fe1b(bipy)] (triangles). (B) $\chi_M T$ versus T plot of freshly prepared crystals of $[Fe1b(bipy)](MeOH)_{0.25}$ (solid squares) and decomposed crystals [Fe1b(bipy)] (open triangels). The loss of included solvent during the grinding process or by long-time storage leads to a reappearance of the thermal hysteresis loop observed for the powder sample. [32b].

HS state. Upon cooling to 125 K, the symmetry of the system is reduced to $P2_1/c$; half of the systematic extinctions observed at 225 K have vanished. Consequently, the asymmetric unit now consists of two iron centers of which one can be assigned to iron(II) in the HS state and the other one to iron(II) in the LS state. A one-dimensional chain of alternating HS and LS iron centers is formed [33]. The only example where a similar structural phase transition is observed is the mononuclear complex [Fe(5-NO_2-sal-N(1,4,7,10))]. Here the formation of two non-equivalent HS and LS sublattices are made responsible for the step in the transition curve [3b]. An examination of the packing of the molecules of [Fe1b(bppa)](MeOH) in the crystal yields a regular solution arrangement of HS and LS molecules, so the same mechanism could be discussed. Recently, Koudriavtsev et al. proposed a quasi-chemical model of specific molecular interactions for the description of step-wise or incomplete spin transitions for mononuclear complexes [40]. A HS → LS transition in a pair of HS molecules with attractively interacting ligands (e.g. hydrogen bonds) involves a relocation of the ligands towards the smaller LS molecule. If the Fe···Fe distances do not follow exactly the changes in Fe–L bonds in the LS species, then the corresponding bond in the HS partner is elongated and thus the HS state is stabilized [40]. This principle can be very easily transferred to polymer chain compounds and the remaining question is, why some of the complexes have a one-step spin transition and others two-step or in other words: are there factors that determine if the Fe···Fe distances can follow exactly the changes in Fe–L bonds or not. The example of the pair [Fe1b(bpea)](MeOH)$_{0.5}$ and [Fe1b(bpea)] with $\Delta T_{1/2}$ = 8 and 28 K, respectively gives the indication that the width of the plateau in the transition curve and also the question of whether a plateau is observed is related to intermolecular interactions. A comparison of the molecule packing of the three complexes [Fe1b(bipy)], [Fe1b(bpea)](MeOH)$_{0.5}$ and [Fe1b(bppa)](MeOH) in the crystal, given in Fig. 10, leads to the assumption that the structure of the polymer chain strongly influences the propagation of the bond length changes along the chain [33]. For the complex [Fe1b(bipy)] an ideal linear chain is obtained and no steps in the transition curve are observed. On the other side, for the complex with the widest step, [Fe1b(bppa)](MeOH) ($\Delta T_{1/2}$ = 76 K), a zigzag structure is observed. The polymer chain structure of [Fe1b(bpea)](MeOH)$_{0.5}$ is somewhere between those two possibilities. It can be easily imagined that for the zigzag structure the Fe···Fe distances cannot follow the Fe–L distance changes so easily compared to linear structures because of restraining interactions (steric hindrance) between the neighboring chains. Next to the zigzag structure, large substituents at the equatorial ligand (L1a instead of L1b) and a dense packing of the molecule chains (absence of solvent molecules) should influence the extent of interactions between the chains and thus the type of spin transition. Indeed, for the only example with an X-ray structure available at the step of the transition curve, [Fe1b(bppa)](MeOH), the change of the Fe···Fe distances is, with an average of 0.20 Å, not so pronounced as the change of the Fe–N(bppa) distances (0.24 Å) upon spin transition [33].

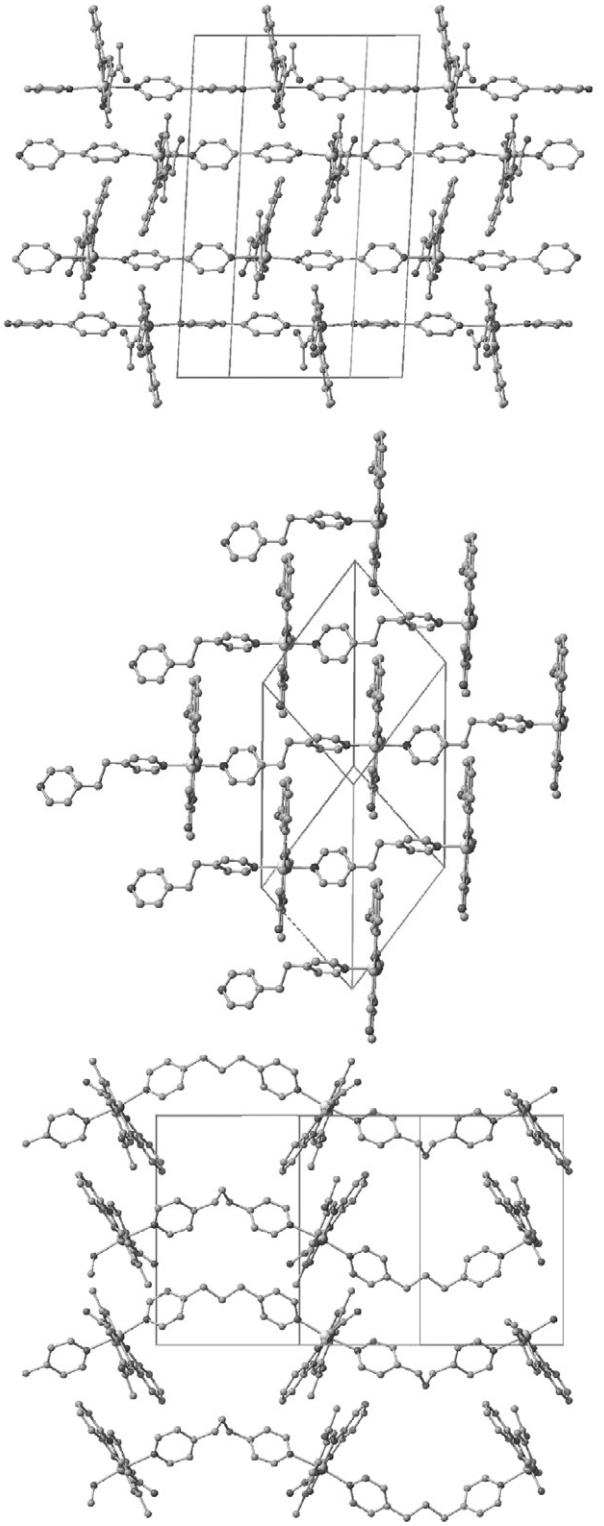

Fig. 10. Side-view of the packing of the molecules in the crystal for the different bridging ligands bipy, bpea and bppa illustrating the differences between linear chains and zigzag chains.

5. Dinuclear complexes

Dinuclear SCO complexes are the simplest system of spin-coupled polymers and the possibility to switch those complexes between the three spin-pair states HS–HS, HS–LS and LS–LS (where HS and LS represent the local high-spin and low-spin states of the dinuclear species) attracted the interest of several research groups [9]. It seems that weak intramolecular interactions are responsible for the direct HS–HS ↔ LS–LS transformation [41], while a plateau in the $\gamma_{HS} \approx 0.5$ (γ_{HS} = HS molar fraction) region might be either due to the intramolecular energetic stabilization of an HS–LS species [37,38] or due to intermolecular interactions [42], The latter possibility leads to continuous transitions in solution.

For the dinuclear complexes of the ligand system discussed in this work, whose properties are summarized in Table 7, incomplete spin transitions are quite frequently observed compared to

Table 7
Overview of octahedral dinuclear iron(II) complexes discussed in this work and their magnetic properties.

	$[Fe_2 2a(L_{ax})_4]$	$[Fe_2 2b(L_{ax})_4]$	$[Fe_2 2c(L_{ax})_4]$	$[Fe_2 2d(L_{ax})_4]$
py	$[Fe_2 2a(py)_4]$ $T_{1/2}$ = 260 K, 90 K, step-wise, incomplete	$[Fe_2 2b(py)_4]$ $T_{1/2}$ = 139 K, incomplete, hysteresis ≈ 8K $[Fe_2 2b(py)_4](py)$ HS/LS	$[Fe_2 2c(py)_4](py)$ HS	$[Fe_2 2d(py)_4]$ $T_{1/2}$ = 175 K, incomplete
phpy	$[Fe_2 2a(phpy)_4](phpy)_2$ $T_{1/2}$ = 215 K, gradual	$[Fe_2 2b(phpy)_4](phpy)$ $T_{1/2}$ = 150 K, gradual, incomplete	–	$[Fe_2 2d(phpy)_4](phpy)_4$ HS
CNpy	$[Fe_2 2a(CNpy)_4](tol)_2$ $T_{1/2}$ = 260 K, gradual	–	–	–
DMAP	$[Fe_2 2a(DMAP)_4]$ HS	$[Fe_2 2b(DMAP)_4]$ $T_{1/2}$ = 150 K, gradual	$[Fe_2 2c(DMAP)_4]$ HS	$[Fe_2 2d(DMAP)_4](DMAP)_4$ HS
1-Meim	$[Fe_2 2a(1\text{-meim})_4]$ HS	$[Fe_2 2b(1\text{-meim})_4](1\text{-meim})_4$ $T_{1/2}$ = 189 K, hysteresis 21 K $[Fe_2 2b(1\text{-meim})_4]$ $T_{1/2}$ = 229 K, gradual	–	–

Table 8
Selected bond lengths [Å] and angles [°] within the first coordination sphere of octahedral dimer iron(II) complexes with the spin state *S*.

Complex	*T* [K]	*S*	Fe–N_{eq}	Fe–O_{eq}	Fe–L_{ax}	O1–Fe–O2	L_{ax}–Fe–L_{ax}	∠ L1, L2[d]	Ref.
$[Fe_2 2a(py)_4](py)$	200	2; 2	2.094(2), 2.098(2)	2.013(2), 2.014(2)	2.264(2), 2.307(2)	110.22(6)		3.9	[43]
$[Fe_2 2b(py)_4](py)_7$	200	2; 2	2.077(3), 2.079(3)	2.006(3), 2.017(3)	2.231(3), 2.289(4)	109.0(1)		36.7	[43]
	125	0	1.899(4), 1.903(4)	1.936(4), 1.939(4)	1.998(5), 2.016(5)	89.8(2)		85.0	
		0	1.895(4), 1.895(4)	1.948(4), 1.950(4)	2.005(5), 2.007(5)	90.2(2)		82.3	
		2	2.087(4), 2.101(4)	2.013(4), 2.036(4)	2.228(5), 2.284(5)	110.8(2)		58.3	
		2	2.092(4), 2.099(4)	2.020(4), 2.034(4)	2.208(5), 2.290(5)	112.2(2)		79.4	
$[Fe_2 2a(1\text{-meim})_4](1\text{-meim})_4$	200	2	2.094(2), 2.112(2)	2.052(2), 2.023(2)	2.217(2), 2.248(2)	111.10(9)	173.94(9)		[24]
$[Fe_2 2b(1\text{-meim})_4](1\text{-meim})_4$	300	2	2.09	2.04	2.25	108	177	45.5	[27]
	125	0	1.902(3), 1.904(3)	1.933(2), 1.944(2)	2.003(3), 2.023(3)	88.24(9)	178.07(10)	44.2	

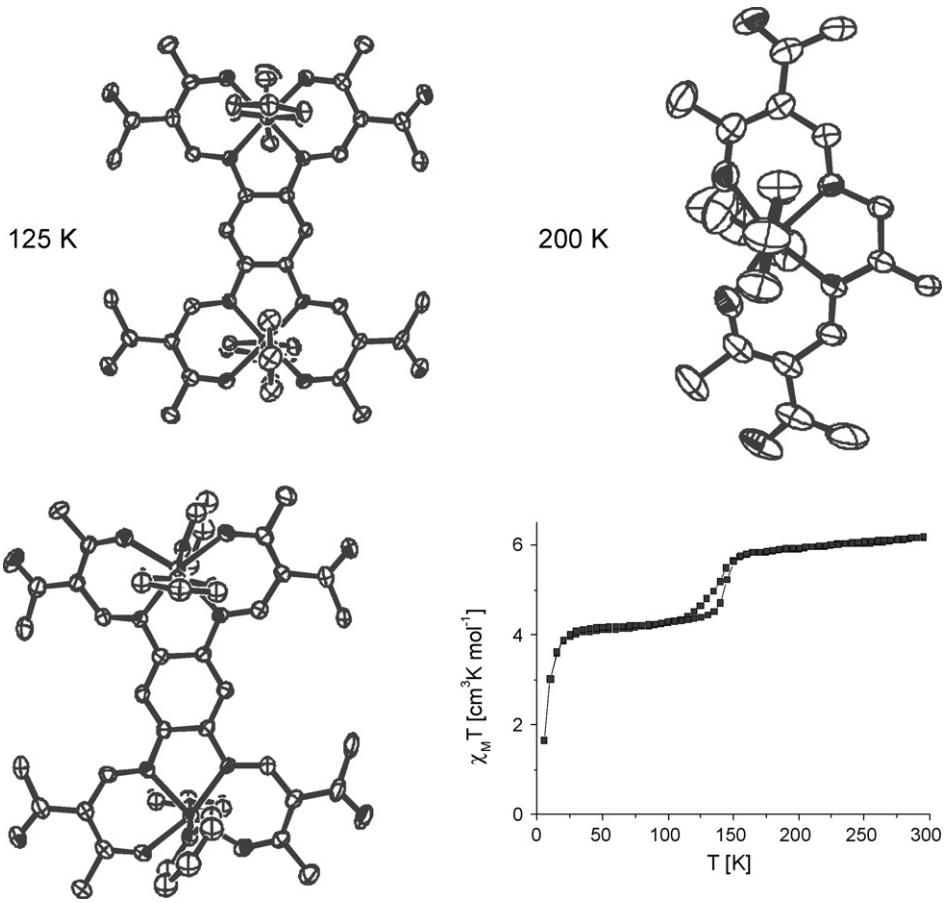

Fig. 11. Magnetism of the dinuclear complex $[Fe_2 2b(py)_4]$ and the top view of the asymmetric unit of single crystals of this compound at 200 and 125 K. In the low-temperature modification, two complex molecules are found in the asymmetric unit, one with both iron centers in the HS state and one with both iron centers in the LS state. Hydrogen atoms and additional solvent molecules are omitted for clarity [43].

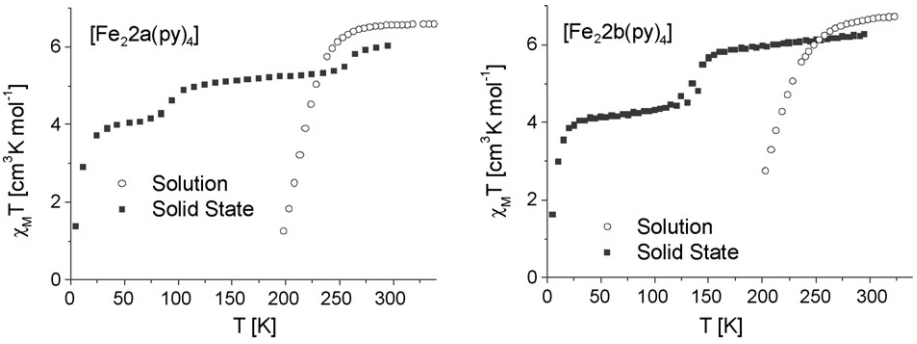

Fig. 12. The magnetism of the dinuclear complex $[Fe_2 2a(py)_4]$ and $[Fe_2 2b(py)_4]$ determined in solution (Evans method) and in the solid state (SQUID measurements). The steps in the $\chi_M T$ versus T curves are clearly due to intermolecular interactions [49].

the mononuclear and polymer systems. However, in contrast to the systems discussed in literature, there is only one example for a complex with a remaining HS molar fraction in the region of $\gamma_{HS} = 0.5$, namely $[Fe_2 2d(py)_4]$ [43]. For the other examples the value is significantly higher ($[Fe_2 2a(py)_4]$: $\gamma_{HS} = 0.67$ at 55 K; $[Fe_2 2b(py)_4]$: $\gamma_{HS} = 0.70$ at 105 K, [43]) or lower ($[Fe_2 2b(phpy)_4](phpy)$: $\gamma_{HS} = 0.28$ at 50 K). This is an indication, probably with the exception of $[Fe_2 2d(py)_4]$, that the incomplete character of the spin transition is not due to an intramolecular stabilization of the mixed HS–LS species but due to intermolecular interactions. A first proof for this theory is the X-ray structure of $[Fe_2 2b(py)_4]$ below the step in the transition curve [43]. Because of the different composition of the single crystals ($[Fe_2 2b(py)_4](py)_7$) and the powder sample ($[Fe_2 2b(py)_4]$) used for the magnetic measurements, for the crystals γ_{HS} is exactly 0.5. Upon spin transition the cell volume of the crystals quadruples and instead of one formula unit per cell, four are found, two of which are crystallographically independent. In Fig. 11, a top view of the asymmetric unit in the HS and in the mixed HS/LS state is given.

Comparison of the bond distances and angles given in Table 8 shows that in one molecule, both iron centers are still in the high-spin state, while in the other molecule, both iron centers are in the low-spin state. The incomplete character of the spin transition is clearly due to intermolecular interactions [43]. As a further argument, the spin transition was also followed in solution using the Evans method [49]. In Fig. 12 the $\chi_M T$ curves obtained in solution are compared with the results from solid state susceptibility measurements for $[Fe_2 2a(py)_4]$ and $[Fe_2 2b(py)_4]$. Both complexes show gradual spin transitions with no indications for steps in the region of $\gamma_{HS} = 0.5$ or 0.7. These results agree with the fact that for pure HS complexes of the same ligand type, only very weak antiferromagnetic interactions between the two iron centers is observed [24]. Those interactions are thought to be responsible for the energetic stabilization of the mixed HS/LS species. The coupling constant obtained, is, with a value around $J = 1–2\ cm^{-1}$, significantly smaller than those reported for other dinuclear complexes, where step-wise spin transitions are obtained quite frequently [9,24].

The two different SCO processes in dinuclear complexes are now well understood, but the question of increasing the cooperative interactions during the spin transition by the use of covalent linkers was eclipsed. To our knowledge there are only two dinuclear complexes with hysteresis, namely $[\{Fe(phdia)_2(NCS)_2\}_2(phdia)]$ (with phdia = 4,7-phenanthroline-5,6-diamine) that shows a step-wise spin transition with a 2 and 7 K wide hysteresis (first and second step, respectively) [37c] and $[(TPyA)Fe(THBQ)Fe(TPyA)](BF_4)_2$ (with TPyA = tris(2-pyridylmethyl)amine; THBQ = 2,3,5,6-tetrahydroxy-1,4-benzoquinonate) that shows a ca. 10 K wide hysteresis [44]. In this context we were able to present a pair of complexes where, by application of a dinucleating chelate ligand, the cooperative interactions during the spin transition increased significantly compared with the mononuclear analog. Due to the higher symmetry of the dinucleating chelate ligand, the number of short intermolecular interactions was doubled and a 3D instead of a 2D network of short intermolecular contacts was formed. This results in an increase of the hysteresis width from 2 K for the mononuclear complex $[Fe1b(1\text{-}meim)_2](1\text{-}meim)$ to 21 K for the dinuclear complex $[Fe_2 2b(1\text{-}meim)_4](1\text{-}meim)_4$ [27]. In Fig. 13 the molecular structure and the results from the magnetic measurement of the two complexes are given.

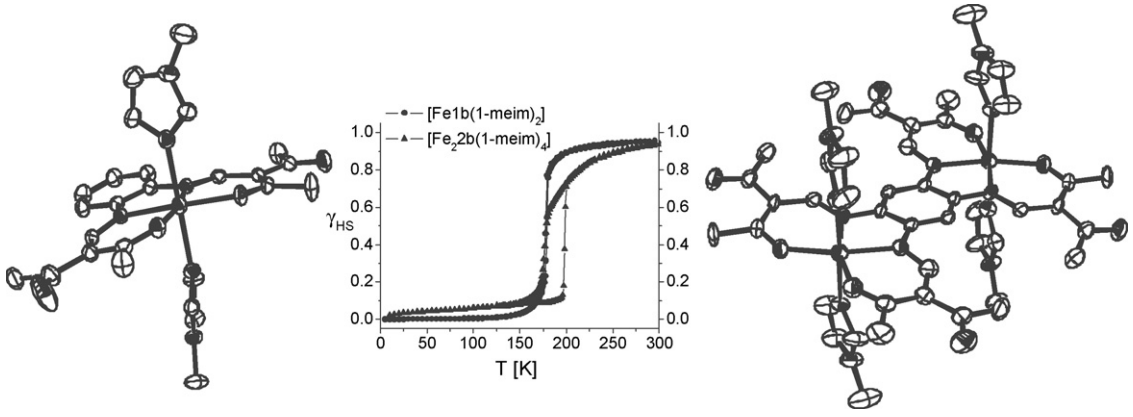

Fig. 13. X-ray structure of the mononuclear complex $[Fe1b(1\text{-}meim)_2](1\text{-}meim)$ and the dinuclear complex $[Fe_2 2b(1\text{-}meim)_4](1\text{-}meim)_4$ and results from the magnetic measurements for the two complexes [27].

6. Characterization in solution

The results obtained for the dinuclear and polymer SCO complexes presented in this work show clearly that it is often difficult to distinguish between the influence of covalent linkers and the influence of intermolecular interactions. For the complexes discussed here it appears that covalent linkers contribute only little to the propagation of elastic interactions. Nevertheless they help to increase the hysteresis width in dinuclear and polymer systems compared to the monomer analogs. It seems that covalent bridges help to optimize the packing of the molecules in a crystal engineering-like approach. In order to more clearly evaluate the influence of the covalent linkers on the abruptness of the transition curve and other packing effects (step-wise or incomplete spin transitions) investigations in solution are necessary where all intermolecular interactions are switched off. The Evans method [45] is one possible means of measuring the susceptibility of paramagnetic compounds in solution. One disadvantage of the Evans method is a relatively high error of 5–10% [46], depending on the concentration of the paramagnetic solute. Additionally, only the bulk susceptibility of the solution is measured and diamagnetic or paramagnetic impurities can lead to incorrect conclusions. This is especially true in the case of air-sensitive iron(II) complexes. Therefore we looked for an alternative technique for investigating iron(II) spin transitions in solution. The application of solution NMR spectroscopy to paramagnetic molecules and biomolecules has been reported for more than 35 years [47]. It was shown to be a useful and sensitive method for detecting changes in the electronic ground state (including spin transitions) in transition metal complexes and there are plenty of textbooks and reviews dealing with this topic [48]. The interpretation of the temperature dependence of the ^{1}H NMR chemical shifts of iron(II) complexes did prove to be a further possibility to follow the spin transition in solution and thereby eliminate some of the disadvantages of the Evans method [49].

For the interpretation of the chemical shifts it is necessary to assign the signals of the spectrum to the different protons of the complex. Due to the different substituents of the complexes discussed in this work, the assignment can be done by spectral comparison and by taking the different line widths into consideration. As one example, the ^{1}H NMR spectrum of [Fe1c(py)$_2$] is given in Fig. 14 with the signal assignment given at the left [49]. This is the only example where we were able to identify all protons of the equatorial ligand. The protons of the axial ligand that are in constant exchange with the non-coordinated molecules are not considered for this investigation, as the axial ligand is normally used in a 50–100 fold excess to ensure the formation of octahedral complexes. The very broad signal of the proton *i* can only be detected in highly concentrated solutions. The signal of proton *h* is often shifted to the diamagnetic region of the spectrum (strongly depending on temperature). If diamagnetic impurities are present or the concentration of the complex is not very high, this signal is also difficult to detect. Those two signals are therefore not considered for the interpretation of the temperature dependence of the NMR shifts [49].

The temperature dependence of the NMR parameters of a pure HS complex [Fe1c(py)$_2$] and a SCO complex [Fe1a(py)$_2$] (isotropic shifts plotted versus $1/T$) is given in part A and B, respectively, of Fig. 15. Above 50 °C (323.15 K; $1/T = 3.1 \times 1000$/K) the behavior of the SCO complexes is similar to the pure HS complexes. At lower temperatures, the isotropic shifts move rapidly towards zero [49]. This behavior can easily be explained by considering the diamagnetic nature of the LS iron(II) center. The spin-flip frequency between the HS and LS state is clearly much faster than the time scale of the NMR experiment. At the beginning of the spin transition the averaged signal of the isotropic shift of the diamagnetic (zero) and the paramagnetic species is measured. Assuming Curie behavior for the high-spin species, the isotropic shift multiplied by the temperature is constant as long as the spin state does not change. A normalized plot of $\delta_{iso} \times T$ versus T should therefore reflect the HS mole fraction (γ_{HS}) of the complex as a function of temperature [49]. Fig. 15C illustrates the corresponding plot for the mononuclear complex [Fe1b(py)$_2$].

The HS mole fraction obtained for the different protons of the complex show significant differences. This is because the paramagnetic shift of the pure HS complex and the SCO complex above 30 °C does not follow the ideal Curie law straight line. This is most probably due to thermally accessible excited states where the d-electrons are rearranged between the two $S = 2$ possibilities ($(d_{xy})^2 (d_{xz}, d_{yz})^2 (d_{z^2})1(d_{x^2-y^2})^1$)and($(d_{xy})^1 (d_{xz}, d_{yz})^3 (d_{z^2})^1 (d_{x^2-y^2})^1$). The experimental data in Fig. 15A and B were fit by taking an

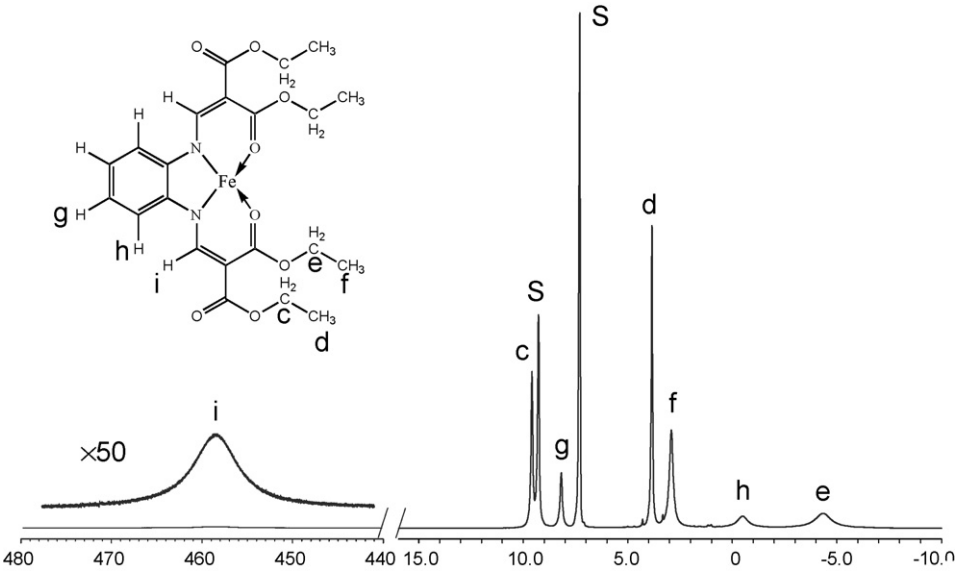

Fig. 14. Proton NMR spectrum of the complex [Fe1c(py)$_2$] in a pyridine at 55 °C. The signal assignment is given at the left. S denotes the solvent pyridine [49].

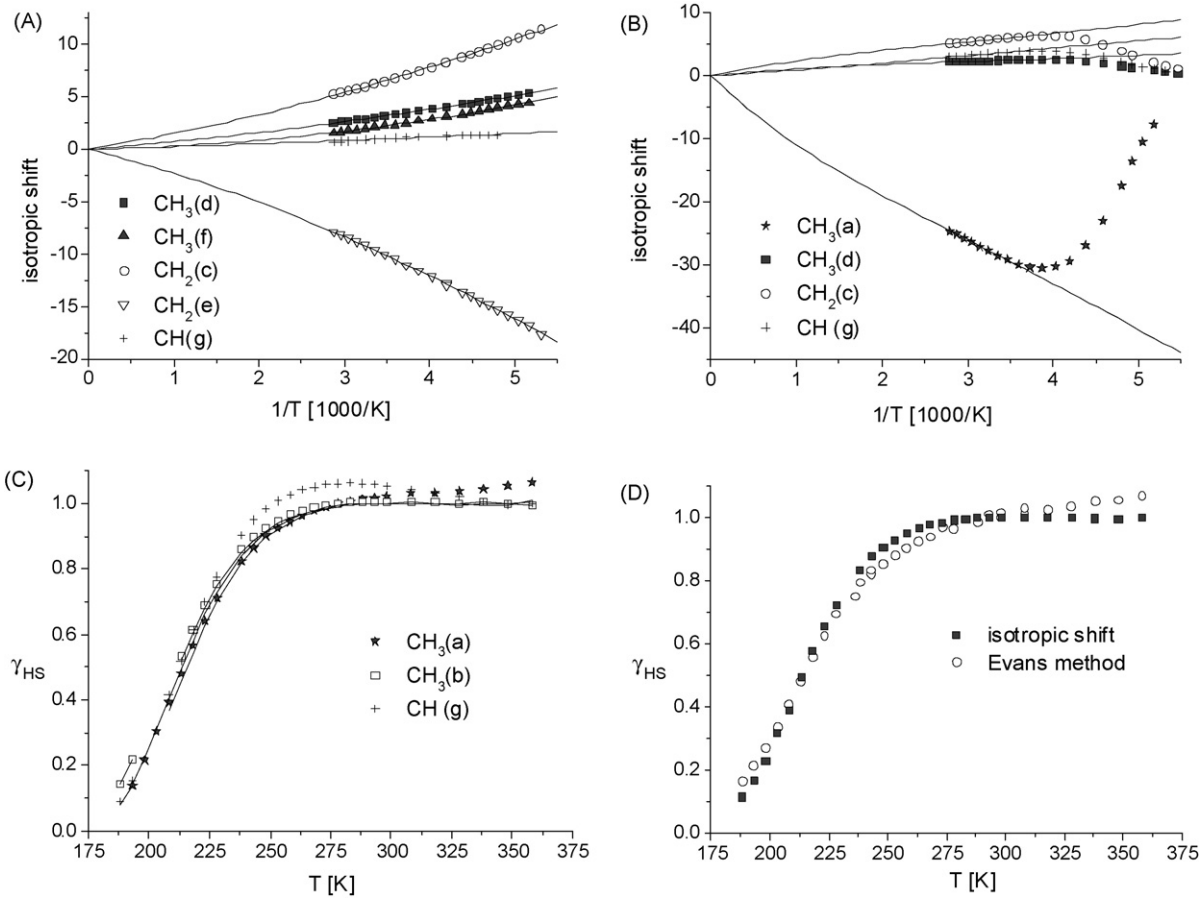

Fig. 15. Isotropic shifts of [Fe1c(py)$_2$] (A) and [Fe1a(py)$_2$] (B) plotted versus 1/*T*. The solid lines represent the calculated shifts of the pure high-spin complex using the extended Curie law [47e]. C shows the HS mole fraction (γ_{HS}) of [Fe1b(py)$_2$] obtained by interpretation of the isotropic shift assuming ideal Curie behavior (points) and using the expanded Curie law (Eq. (1)) for the temperature dependence of the high-spin species. In D the high-spin mole fraction of [Fe1b(py)$_2$] obtained by interpretation of the isotropic shifts and using the Evans method are compared. Good agreement between the two methods is observed [49].

extended Curie law into account with different Curie constants (or spin densities) for the ground and exited states [46e]:

$$\delta_n^{con} = \left(\frac{F}{T}\right) \frac{\left\{W_1 C_{n1}^2 + W_2 C_{n2}^2 e^{-\Delta E/kT}\right\}}{\left\{W_1 + W_2 e^{-\Delta E/kT}\right\}} \quad (1)$$

where W_1 and W_2 are the weighting factors for the ground and excited state ($S(S+1)$ in each case), C_{n1} and C_{n2} are the orbital coefficients (spin densities) for ground state and excited state, F is the Curie constant, ΔE is the energy difference between the ground state and the first excited state and k is the Boltzmann constant. The calculated isotropic shifts for the pure HS complex [Fe1b(py)$_2$] at lower temperature can now be used to more accurately determine the HS molar fraction (γ_{HS}) of the complex as function of temperature according to

$$\gamma_{HS} = \frac{(\delta^{con}(\text{measured})T)}{(\delta^{con}(\text{calculated})T)} \quad (2)$$

The results are given as solid lines in Fig. 15C. In Fig. 15D the average of the spin transition curves obtained by interpretation of the NMR resonances is compared with the transition curve obtained by the Evans method for the mononuclear complex [Fe1b(py)$_2$]. A good agreement is observed.

Several disadvantages must be taken into account when using the Evans method: the exact concentration of the paramagnetic solute must be determined to high accuracy and for air-sensitive complexes and considering the small quantities used, very careful work is required. The method determines the bulk susceptibility of the solution, and impurities are difficult to detect and can lead to erroneous results. The inner capillary should be fixed properly and a suitable inert reference substance must be used. Taking all these points into consideration, the information obtained is at least of the same, and usually of much higher quality. Besides, the samples are much easier to prepare. The main disadvantage of this method is the necessity of assigning at least some of the resonances in the NMR spectrum in order to correct the observed shift by its diamagnetic fraction. On the other hand, successful signal assignment makes it clear whether the investigated species is still intact in solution. This is particularly important for dinuclear complexes with bridging ligands where dissociation into monomers might occur. Last but not least, both methods can be applied in parallel in the same series of experiments, and thereby combine the advantages of both. So far we only investigated monomer and dimer SCO complexes in solution. The obtained transition curves give no indication for an increase of cooperative interactions for the dinuclear complexes [27,49]. The same can be said about steps in the transition curve or incomplete spin transitions. However, the method can be used to make predictions if certain combinations of equatorial and axial ligands are suitable for the synthesis of SCO complexes. Using this method we were recently able to follow a spin transition of a negatively charged SCO complex of this ligand type using cyanide or rhodanide as axial ligands. This is, to our

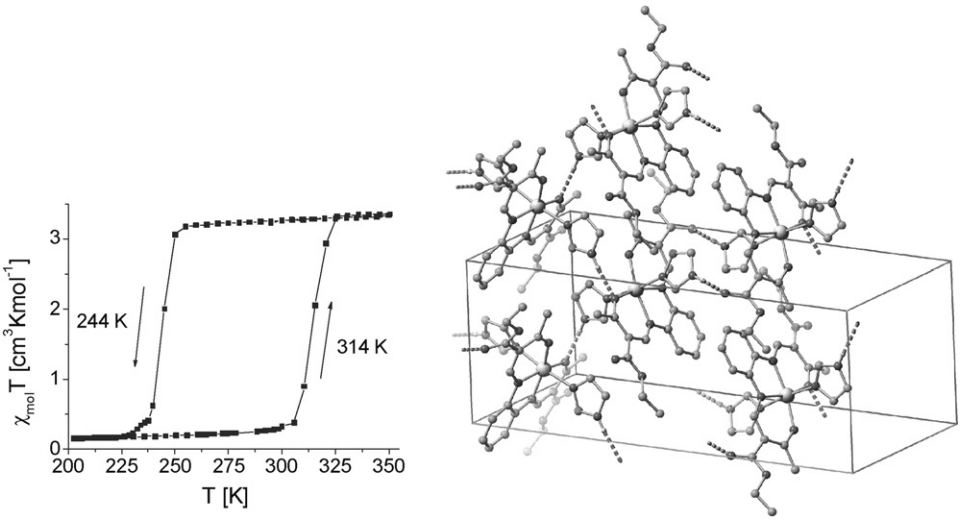

Fig. 16. X-ray structure and results from the magnetic measurements for the complexes [Fe1a(Him)$_2$] [50].

knowledge, the first example for a negatively charged SCO complex [50].

7. Conclusion and prospectives

The magnetic properties and results from X-ray structure analysis of several monomer, dimer and polymer iron(II) spin crossover complexes are discussed in this article. Special attention has been given to the possibility of increasing cooperative interactions by the application of covalent linkers. However, although an increase in the hysteresis width can be observed when going from monomer to dimer or polymer systems, a closer examination of the different structures, a comparison of the results with results from literature and finally investigations in solution clearly demonstrated that the increase of the cooperative interactions during the spin transition is mainly due to an increased number of intermolecular contacts. The covalent linkers, most likely, do not have the ability to transmit the geometric changes associated with the spin transition through the crystal lattice and, by this, increase the cooperative interactions. This does not imply that those linkers are useless. The results show that they can be used to optimize the packing of the molecules in the crystal in a crystal engineering-like approach. For this purpose rigid linkers are most suited. Next to spin transitions with wide thermal hysteresis loops around room temperature, step-wise spin transitions are also of interest because of the possibility of addressing more than two different states. As in the discussions about the cooperative interactions, the factor determining the presence or absence of steps in the transition curve is again the packing of the molecules in the crystals. No evidence was found for the appearance of step-wise spin transitions due to a intramolecular stabilization of [HS–LS] pairs as frequently observed for other systems [9]. Interestingly, the intermolecular interactions for both phenomena are very similar (short intermolecular contacts) and only the question of whether the arrangement of the molecules in the crystal promotes or hinders the shortening of the Fe···Fe distances, in line with the shortening of the Fe–L distances upon spin transition, is the difference.

The aim of future investigations is now to optimize the intermolecular interactions to obtain wide hysteresis loops. Two factors can be improved: on the one side there are the number and dimension of the intermolecular contacts—here a limit in the hysteresis width is already visible as even for systems with 3D networks of short van der Waals contacts no hysteresis loops wider than 20 K were observed. The second point is the type of interactions. So far only weak or non-classical hydrogen bonds in combination with some additional short van der Waals contacts were observed for the complexes under investigation. One possibility to improve the ligand system would be to provide preconditions for π-stacking interactions. Those are responsible for the widest hysteresis loops observed so far for structurally characterized complexes [34]. Recently we found however, the indication that hydrogen bonds might also be very suitable for the transmission of cooperative interactions [51]. An iron(II) complex of the ligand L1a with imidazole as axial ligands gives a spin transition complex with a 70 K wide thermal hysteresis loop. Results from X-ray structure analysis show that a 2D network of hydrogen bonds is formed between the imidazole NH and the carbonyl oxygen of the equatorial ligand as given in Fig. 16. Consequently, the ligand system now will be modified in order to introduce suitable hydrogen bond donors to prove this theory.

Acknowledgements

This work has been supported financially by the Deutsche Forschungsgemeinschaft (SPP 1137), the Fonds der Chemischen Industrie and the Center for Integrated Protein Science Munich CIPSM. For the acquisition of the Mössbauer spectra the author thanks K. Achterhold and F. Parak, Technical University Munich, H. Paulen, University Lübeck and P. Gütlich, University Mainz. The photomagnetic investigations were performed in cooperation with J.-F. Letard, ICMCB Bordeaux and the NMR investigation in cooperation with F. Ann Walker, University of Arizona, Tucson. For the acquisition of the data for X-ray structure analysis the author thanks P. Mayer and S. Albrecht, University of Munich. The synthesis of the complexes was mainly done by E. Kaps, W. Bauer and J. Obel with the help of several undergraduate students.

References

[1] (a) H.A. Goodwin, Coord. Chem. Rev. 18 (1976) 293;
(b) P. Gütlich, Struct. Bonding (Berlin) 44 (1981) 83;
(c) E. König, Prog. Inorg. Chem. 35 (1987) 527;
(d) P. Gütlich, A. Hauser, Coord. Chem. Rev. 97 (1990) 1;
(e) E. König, Struct. Bonding (Berlin) 76 (1991) 51;
(f) P. Gütlich, A. Hauser, H. Spiering, Angew. Chem. Int. Ed. Engl. 33 (1994) 2024;
(g) P. Gütlich, J. Jung, H. Goodwin, in: E. Coronado, P. Delhaes, D. Gatteschi, J.S.

Miller (Eds.), NATO ASI Series E: Applied Sciences, vol. 321, Kluwer Academic Publishing, 1996, p. 327;
(h) P. Gütlich, H.A. Goodwin (Eds.), Spin Crossover in Transition Metal Compounds I—III, Topics in Current Chemistry, Springer-Verlag, Berlin, Heidelberg, New York, 2004;
(i) J.A. Real, A.B. Gaspar, M.C. Munoz, Dalton Trans. (2005) 2062;
(j) O. Sato, J. Tao, Y.-Z. Zhang, Angew. Chem. 119 (2007) 2200;
(k) O. Sato, J. Tao, Y.-Z. Zhang, Angew. Chem. Int. Ed. 46 (2007) 2152.
[2] (a) O. Kahn, C. Jay Martinez, Science 279 (1998) 44;
(b) O. Kahn, C. Jay, J. Kröber, R. Claude, F. Grolière, Patent EP0666561 (1995).;
(c) J.-F. Létard, O. Nguyen, N. Daro, Patent FR0512476 (2005);
(d) J.-F. Létard, P. Guionneau, L. Goux-Capes, in: P. Gütlich, H.A. Goodwin (Eds.), Topics in Current Chemistry, vol. 235, Springer, Wien, New York, 2004, p. 221;
(e) A. Galet, A.B. Gaspar, M.C. Munoz, G.V. Bukin, G. Levchenko, J.A. Real, Adv. Mater. 17 (2005) 2949.
[3] (a) G. Psomas, N. Bréfuel, F. Dahan, J.-P. Tuchagues, Inorg. Chem. 43 (2004) 4590;
(b) D. Boinnard, A. Bousseksou, A. Dworkin, J.-M. Savariault, F. Varret, J.-P. Tuchagues, Inorg. Chem. 33 (1994) 271;
(c) L. Salmon, A. Bousseksou, B. Donnadieu, J.-P. Tuchagues, Inorg. Chem. 44 (2005) 1763.
[4] V.A. Grillo, L.R. Gahan, G.R. Hanson, R. Stranger, T.W. Hambley, K.S. Murray, B. Moubaraki, J.D. Cashion, J. Chem. Soc., Dalton Trans. (1998) 2341.
[5] J.S. Costa, C. Balde, C. Carbonera, D. Denux, A. Wattiaux, C. Desplanches, J.P. Ader, P. Gütlich, J.-F. Létard, Inorg. Chem. 46 (2007) 4114.
[6] (a) M. Nelson, P.D.A. McIlroy, C.S. Stevenson, E. König, G. Ritter, J. Waigel, J. Chem. Soc. Dalton Trans. (1986) 991;
(b) E. König, G. Ritter, J. Dengler, M. Nelson, Inorg. Chem. 26 (1987) 3582;
(c) S. Hayami, Z.-Z. Gu, Y. Einaga, Y. Kobayashi, Y. Ishikawa, Y. Yamada, A. Fujishima, O. Sato, Inorg. Chem. 40 (2001) 240;
(d) J.S. Costa, P. Guionneau, J.-F. Létard, J. Phys.: Conf. Ser. 21 (2005) 67;
(e) P. Guionneau, F. Le Gac, A. Kaiba, J.S. Costa, J.-F. Létard, Chem. Commun. (2007) 3723.
[7] (a) O. Kahn, E. Codjovi, Philos. Trans. R. Soc. London, Ser. A 354 (1996) 359;
(b) O. Kahn, Y. Garcia, J.-F. Létard, C. Mathoniére, NATO ASI Ser., Ser. C 518 (1998) 127.
[8] (a) C. Genre, G.S. Matouzenko, E. Jeanneau, D. Luneau, New J. Chem. 30 (2006) 1669;
(b) P.J. van Koningsbruggen, Y. Garcia, O. Kahn, L. Fournés, H. Kooijman, A.L. Spek, J.G. Haasnoot, J. Moscovici, K. Provost, A. Michalowicz, F. Renz, P. Gütlich, Inorg. Chem. 39 (2000) 1891;
(c) N. Moliner, M.C. Munoz, S. Létard, L. Salmon, J.-P. Tuchagues, A. Bousseksou, J.A. Real, Inorg. Chem. 41 (2002) 6997;
(d) J.A. Real, E. Andrés, M.C. Munoz, M. Julve, T. Granier, A. Bousseksou, F. Varret, Science 268 (1995) 265;
(e) N. Moliner, M.C. Munoz, S. Létard, X. Solans, N. Menéndez, A. Goujon, F. Varret, J.A. Real, Inorg. Chem. 39 (2000) 5390;
(f) G.S. Matouzenko, G. Molnár, N. Bréfuel, M. Perrin, A. Bousseksou, S.A. Borshch, Chem. Mater. 15 (2003) 550;
(g) Y. Garcia, V. Niel, M.C. Munoz, J.A. Real, Top. Curr. Chem. 233 (2004) 229;
(h) G.S. Matouzenko, M. Perrin, B. Le Guennic, C. Genre, G. Molnár, A. Bousseksou, S.A. Borshch, Dalton Trans. (2007) 934;
(i) J.A. Real, A.B. Gaspar, V. Niel, M.C. Munoz, Coord. Chem. Rev. 236 (2003) 121;
(j) S.M. Neville, B.A. Leita, D.A. Offermann, M.B. Duriska, B. Moubaraki, K.W. Chapman, G.J. Halder, K.S. Murray, Eur. J. Inorg. Chem. (2007) 1073;
(k) K.S. Murray, C.J. Kepert, Top. Curr. Chem. 233 (2004) 195.
[9] A. Bousseksou, G. Molnár, J.A. Real, K. Tanaka, Coord. Chem. Rev. 251 (2007) 1822 (and references therein).
[10] (a) E.-G. Jäger, in: L. Fabbrizzi, A. Poggi (Eds.), Chemistry at the Beginning of the Third Millennium, Springer-Verlag, Berlin, Heidelberg, New York, 2000, p. 103;
(b) E.-G. Jäger, J. Knaudt, K. Schuhmann, A. Guba, in: W. Adam (Ed.), Peroxide Chemistry—Mechanistic and Preparative Aspects of Oxygen Transfer, Wiley-VCH, Weinheim, 2000, p. 249;
(c) E.-G. Jäger, St. Barth, H. Keutel, F. Wiesemann, U. Gaudig, in: A.X. Trautwein (Ed.), Bioinorganic Chemistry—Transition Metals in Biology and their Coordination Chemistry, Wiley-VCH, Weinheim, 1997, p. 584.
[11] (a) B. Weber, I. Käpplinger, H. Görls, E.-G. Jäger, Eur. J. Inorg. Chem. (2005) 2794.
[12] (a) R. Wegner, M. Gottschaldt, H. Görls, E.-G. Jäger, D. Klemm, Chem. Eur. J. 7 (2001) 2143;
R. Wegner, M. Gottschaldt, H. Görls, E.-G. Jäger, D. Klemm, Angew. Chem. 112 (2000) 608;
R. Wegner, M. Gottschaldt, H. Görls, E.-G. Jäger, D. Klemm, Angew. Chem. Int. Ed. 39 (2000) 595;
(b) H. Keutel, H. Görls, W. Poppitz, A. Schütz, E.-G. Jäger, J. Prakt. Chem. 341 (1999) 785;
(c) H. Elias, D. Hess, H. Paulus, E.-G. Jäger, F. Gräfe, Z. anorg. allg. Chem. 101 (1990) 101;
(d) E.-G. Jäger, K. Müller, Z. anorg. allg. Chem. 526 (1985) 29;
(e) E.-G. Jäger, K. Müller, Z. anorg. allg. Chem. 482 (1981) 201.
[13] (a) Y. Nishida, K. Hayashida, N. Oishi, S. Kida, Inorg. Chim. Acta 38 (1980) 213;
(b) W.W. Minin, Yu.W. Rakitin, G.M. Larin, E.-G. Jäger, Zh. Neorg. Khim. 26 (1981) 650.
[14] (a) D.G. Pillsbury, D.H. Busch, J. Am. Chem. Soc. 98 (1981) 7836;
(b) J.A. Streeky, D.G. Pillsbury, D.H. Busch, Inorg. Chem. 19 (1980) 3148;
(c) Yu.E. Kovalenko, Ya.D. Lampeka, I. Ya. Levitin, K.B. Yatsimirkii, K. Müller, D. Seidel, E.-G. Jäger, Russ. Chem. Bull. 42 (1993) 981;
(d) E.-G. Jäger, H. Keutel, M. Rudolph, B. Krebs, F. Wiesemann, Chem. Ber. 128 (1995) 503.
[15] (a) E.-G. Jäger, M. Rudolph, R. Müller, Z. Chem. 18 (1978) 229;
(b) E.-G. Jäger, P. Renner, R. Schmidt, Z. Chem. 18 (1978) 193;
(c) E.-G. Jäger, B. Kirchhof, E. Schmidt, B. Remde, A. Kipke, R. Müller, Z. anorg. allg. Chem. 485 (1982) 141;
(d) E.-G. Jäger, G. Schlenvoigt, B. Kirchhof, M. Rudolph, R. Müller, Z. anorg. allg. Chem. 485 (1982) 173;
(e) E.-G. Jäger, K. Schuhmann, H. Görls, Inorg. Chim. Acta 255 (1997) 295;
E.-G. Jäger, K. Schuhmann, H. Görls, Chem. Ber./Recueil 130 (1997) 1643;
(f) K. Schuhmann, E.-G. Jäger, Eur. J. Inorg. Chem. (1998) 2051.
[16] (a) K. Kubokura, H. Okawa, S. Kida, Bull. Chem. Soc. Jpn. 51 (1978) 2036;
(b) G.W. Larin, W.W. Minin, E.-G. Jäger, P. Renner, Zh. Neorg. Khim. 25 (1980) 183;
(c) E.-G. Jäger, K. Müller, Z. anorg. allg. Chem. 501 (1983) 40;
(d) E.-G. Jäger, J. Knaudt, M. Rudolph, M. Rost, Chem. Ber. 129 (1996) 1041;
(e) J. Knaudt, St. Förster, U. Bartsch, A. Rieker, E.-G. Jäger, Z. Naturforsch. 55b (2000) 86;
(f) R. Wegner, M. Gottschaldt, W. Poppitz, E.-G. Jäger, D. Klemm, J. Mol. Catal. A: Chem. 201 (2003) 91;
(g) M. Rudolph, S. Dautz, E.-G. Jäger, J. Am. Chem. Soc. 44 (2000) 10821;
(h) E.-G. Jäger, D. Seidel, M. Rudolph, A. Schneider, Z. Chem. 26 (1986) 76;
(i) H. Görls, G. Reck, E.-G. Jäger, K. Müller, D. Seidel, Cryst. Res. Technol. 25 (1990) 1277.
[17] B. Weber, E.-G. Jäger, Eur. J. Inorg. Chem., accepted, doi:10.1002/ejic.200800891.
[18] E.-G. Jäger, E. Häussler, M. Rudolph, A. Schneider, Z. anorg. allg. Chem. 525 (1985) 67.
[19] (a) B. Weber, H. Görls, M. Rudolph, E.-G. Jäger, Inorg. Chim. Acta 337 (2002) 47;
(b) B. Weber, Dissertation, Ph.D. Thesis, 2002, Universität Jena, Germany, Der Andere Verlag, 2003.
[20] G. Leibeling, Ph.D. Thesis, University of Jena/Germany, 2003.
[21] B. Weber, E. Kaps, J. Weigand, C. Carbonera, J.-F. Letard, K. Achterhold, F.-G. Parak, Inorg. Chem. 47 (2008) 487.
[22] H. Görls, E.-G. Jäger, Cryst. Res. Technol. 26 (1991) 349.
[23] B. Weber, E.S. Kaps, C. Desplanches, J.-F. Létard, K. Achterhold, F.G. Parak, Eur. J. Inorg. Chem. (2008) 4891.
[24] W. Bauer, B. Weber, Inorg. Chim. Acta, accepted, doi:10.1016/j.ica.2008.10.018.
[25] B. Weber, C. Carbonera, C. Desplanches, J.-F. Létard, Eur. J. Inorg. Chem. (2008) 1589.
[26] B. Weber, E.S. Kaps, J. Obel, W. Bauer, Z. Anorg. Allg. Chem. (2008) 1421.
[27] B. Weber, E.S. Kaps, J. Obel, K. Achterhold, F.G. Parak, Inorg. Chem., doi:10.1021/ic801388a, in press.
[28] K.F. Purcell, M.P. Edwards, Inorg. Chem. 23 (1984) 2620.
[29] (a) S. Marcen, L. Lecren, L. Capes, H.A. Goodwin, J.-F. Létard, Chem. Phys. Lett. 358 (2002) 87;
(b) J.-F. Létard, P. Guionneau, O. Nguyen, J.S. Costa, S. Marcén, G. Chastanet, M. Marchivie, L. Capes, Chem. Eur. J. 11 (2005) 4582.
[30] (a) A. Hauser, Coord. Chem. Rev. 111 (1991) 275;
(b) A. Hauser, J. Jeftic, H. Romstedt, R. Hinek, H. Spiering, Coord. Chem. Rev. 190–192 (1999) 471.
[31] (a) J.-F. Létard, P. Guionneau, L. Rabardel, J.A.K. Howard, A.E. Goeta, D. Chasseau, O. Kahn, Inorg. Chem. 37 (1998) 4432;
(b) J.-F. Létard, G. Chastanet, O. Nguyen, S. Marcen, M. Marchivie, P. Guionneau, D. Chasseau, P. Gütlich, Monatsh. Chem. 134 (2003) 165;
(c) J.-F. Létard, J. Mater. Chem. 16 (2006) 2550.
[32] (a) B. Weber, R. Tandon, D. Himsl, Z. Anorg. Allg. Chem. 633 (2007) 1159;
(b) B. Weber, E.S. Kaps, C. Desplanches, J.-F. Létard, Eur. J. Inorg. Chem. (2008) 2963.
[33] W. Bauer, W. Scherer, C. Kurth, B. Weber, in preparation.
[34] (a) J.-F. Létard, P. Guionneau, E. Codjovi, O. Lavastre, G. Bravic, D. Chasseau, O. Kahn, J. Am. Chem. Soc. 119 (1997) 10861;
(b) Z.J. Zhong, J.-Q. Tao, Z. Yu, C.-Y. Dun, Y.-J. Lui, X.-Z. You, J. Chem. Soc., Dalton Trans. (1998) 327;
(c) S. Hayami, Z.-z. Gu, H. Yoshiki, A. Fujishima, O. Sato, J. Am. Chem. Soc. 123 (2001) 11644;
(d) J.-F. Létard, L. Capes, G. Chastanet, N. Moliner, S. Létard, J.-A. Real, O. Kahn, Chem. Phys. Lett. 313 (1999) 115;
(e) H. Daubric, C. Cantin, C. Thomas, J. Kliava, J.-F. Létard, O. Kahn, Chem. Phys. 244 (1999) 75.
[35] (a) Y. Miyazaki, T. Nakamoto, S. Ikeuchi, K. Saito, A. Inaba, M. Sorai, T. Tojo, T. Atake, G.S. Matouzenko, S. Zein, S.A. Borshch, J. Phys. Chem. B 111 (2007) 12508;
(b) E. König, G. Ritter, S.K. Kulshreshtha, N. Csatary, Inorg. Chem. 23 (1984) 1903;
(c) E. König, G. Ritter, S.K. Kulshreshtha, Inorg. Chem. 23 (1984) 1144;
(d) E.W. Müller, H. Spiering, P. Gütlich, Chem. Phys. Lett. 93 (1982) 567;
(e) M.S. Haddad, W.D. Federer, M.W. Lynch, D.N. Hendrickson, Inorg. Chem. 20 (1981) 131.
[36] (a) Y. Garcia, O. Kahn, L. Rabardel, B. Chansou, L. Salmon, J.-P. Tuchagues, Inorg. Chem. 38 (1999) 4663;
(b) G.S. Matouzenko, J.-F. Letard, S. Lecocq, A. Bousseksou, L. Capes, L. Salmon, M. Perrin, O. Kahn, A. Collet, Eur. J. Inorg. Chem. (2001) 2935;
(c) W. Hibbs, P.J. van Koningsbruggen, A.M. Arif, W.W. Shum, J.S. Miller, Inorg. Chem. 42 (2003) 5645;

(d) P. Poganiuch, S. Decurtins, P. Gütlich, J. Am. Chem. Soc. 112 (1990) 3270;
(e) L. Wiehl, Acta Crystallogr., Sect. B 49 (1993) 289;
(f) R. Hinek, H. Spiering, D. Schollmeyer, P. Gütlich, A. Hauser, Chem. Eur. J. 2 (1996) 1427.
[37] (a) J.A. Real, A.B. Gaspar, M.C. Munoz, P. Gütlich, V. Ksenofontov, H. Spiering, in: P. Gütlichet, H.A. Goodwin (Eds.), Topics in Current Chemistry, vol. 233, Springer, Wien, New York, 2004, p. 167;
(b) A.B. Gaspar, M.C. Munoz, J.A. Real, J. Mater. Chem. (2006) 2522;
(c) V. Ksenofontov, A.B. Gaspar, V. Niel, S. Reiman, J.A. Real, P. Gütlich, Chem. Eur. J. 10 (2004) 1291.
[38] (a) S. Zein, S.A. Borshch, J. Am. Chem. Soc. 127 (2005) 16197;
(b) K. Nakano, S. Kawata, K. Yoneda, A. Fuyuhiro, T. Yagi, S. Nasu, S. Morimoto, S. Kaizaki, Chem. Commun. (2004) 2892.
[39] (a) M. Mikami, M. Konno, Y. Saito, Chem. Phys. Lett. 63 (1979) 566;
(b) N. Sasaki, T. Kambara, Phys. Rev. B 40 (1989) 2442;
(c) A. Bousseksou, J. Nasser, J. Linares, K. Boukheddaden, F. Varret, J. Phys. 12 (1992) 1381;
(d) H. Spiering, T. Kohlhaas, H. Romstedt, A. Hauser, C. Bruns-Yilmaz, P. Gütlich, Coord. Chem. Rev. 190–192 (1999) 629;
(e) V. Petrouleas, J.-P. Tuchagues, Chem. Phys. Lett. 137 (1987) 21;
(f) D. Boinnard, A. Bousseksou, A. Dworkin, J.-M. Savariault, F. Varret, J.-P. Tuchaugues, Inorg. Chem. 33 (1994) 271.
[40] (a) A.B. Koudriavtsev, A.F. Strassen, J.G. Haasnoot, M. Grunert, P. Weinberger, W. Linert, Phys. Chem. Chem. Phys. 5 (2003) 3676;
(b) A.B. Koudriavtsev, A.F. Strassen, J.G. Haasnoot, M. Grunert, P. Weinberger, W. Linert, Phys. Chem. Chem. Phys. 5 (2003) 3666.
[41] A.B. Gaspar, V. Ksenofontov, J.A. Real, P. Gütlich, Chem. Phys. Lett. 373 (2003) 385.
[42] N. Ortega-Villar, A.L. Thompson, M.C. Munoz, V.M. Ugalde-Sadivar, A.E. Goeta, R. Moreno-Esparza, J.A. Real, Chem. Eur. J. 11 (2005) 5721.
[43] B. Weber, E. Kaps, Heteroatom Chem. 16 (2005) 391.
[44] K.S. Min, K. Swierczek, A.G. DiPasquale, A.L. Rheingold, W.M. Reiff, A.M. Arif, J.S. Miller, Chem. Commun. (2008) 317.
[45] (a) D.F.J. Evans, J. Chem. Soc. (1959) 2003;
(b) D.H. Live, S.I. Chan, Anal. Chem. 42 (1970) 791;
(c) D. Ostfeld, I.A. Cohen, J. Chem. Educ. 49 (1972) 829;
(d) E.M. Schubert, Chem. Educ. 69 (1992) 62.
[46] L.A. Yatsunyk, F.A. Walker, Inorg. Chem. 43 (2004) 757.
[47] (a) G.N. La Mar, W.D. Horrocks, R.H. Holm (Eds.), NMR in Paramagnetic Molecules, Academic Press, New York, 1973;
(b) G.N. La Mar, F.A. Walker, in: D. Dolphin (Ed.), The Porphyrins, vol. IV, Academic Press, NY, 1979, p. 61;
(c) I. Bertini, C. Luchinat, G. Parigi, Solution NMR of Paramagnetic Molecules, Springer-Verlag, Heidelberg, 2001;
(d) F.H. Köhler, in: J.S. Miller, M. Drillon (Eds.), Magnetism: Molecules to Materials. Models and Experiments, Wiley-VCH, Weinheim, 2001, p. 379;
(e) F.A. Walker, in: K.M. Kadish, K.M. Smith, R. Guilard (Eds.), The Porphyrin Handbook, vol. 5, Academic Press, London, 2000, p. 81.
[48] (a) G.N. La Mar, F.A. Walker, in: D. Dolphin (Ed.), The Porphyrins, vol. IV, Academic Press, NY, 1979, p. 61;
(b) I. Bertini, C. Luchinat, G. Parigi, Solution NMR of Paramagnetic Molecules, Springer-Verlag, Heidelberg, 2001;
(c) F.H. Köhler, in: J.S. Miller, M. Drillon (Eds.), Magnetism: Molecules to Materials. Models and Experiments, Wiley-VCH, Weinheim, 2001, p. 379.
[49] B. Weber, F.A. Walker, Inorg. Chem. 46 (2007) 6794.
[50] (a) B. Weber, J. Schulten, in preparation.
[51] B. Weber, W. Bauer, J. Obel, Angew. Chem. Int. Ed., doi:10.1002/anie.200802806, in press.